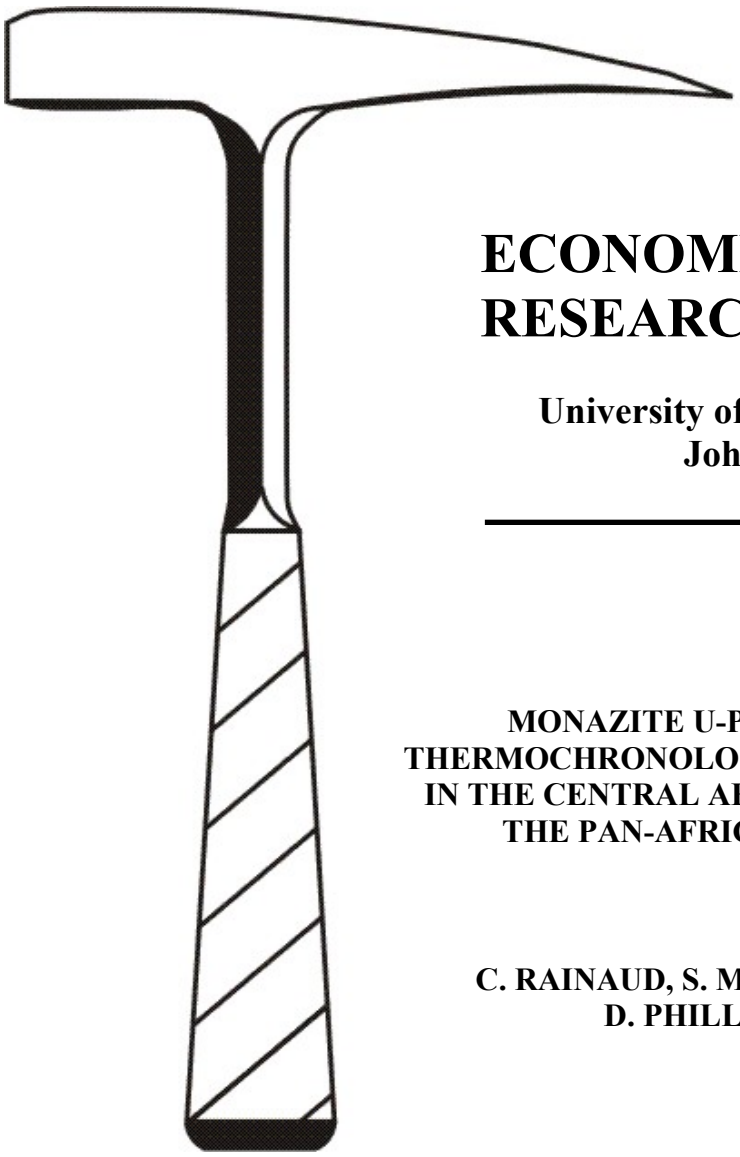

ECONOMIC GEOLOGY RESEARCH INSTITUTE

University of the Witwatersrand
Johannesburg

MONAZITE U-PB DATING AND ^{40}AR-^{39}AR THERMOCHRONOLOGY OF METAMORPHIC EVENTS IN THE CENTRAL AFRICAN COPPERBELT DURING THE PAN-AFRICAN LUFILIAN OROGENY

C. RAINAUD, S. MASTER, R. A. ARMSTRONG, D. PHILLIPS AND L. J. ROBB

INFORMATION CIRCULAR No. 391

UNIVERSITY OF THE WITWATERSRAND
JOHANNESBURG

MONAZITE U-PB DATING AND ^{40}AR-^{39}AR THERMOCHRONOLOGY OF METAMORPHIC EVENTS IN THE CENTRAL AFRICAN COPPERBELT DURING THE PAN-AFRICAN LUFILIAN OROGENY

by

C. RAINAUD[a], S. MASTER[a], R. A. ARMSTRONG[b], D. PHILLIPS[c] AND L. J. ROBB[a]

[a] Economic Geology Research Institute, School of Geosciences, University of the Witwatersrand, P. Bag 3, WITS 2050, South Africa.
christinerainaud@hotmail.com
[b] PRISE, Research School of Earth Sciences, Australian National University, Canberra, Australia
[c] School of Earth Sciences, University of Melbourne, Melbourne, Victoria, Australia

ECONOMIC GEOLOGY RESEARCH INSTITUTE
INFORMATION CIRCULAR No. 391

August, 2005

MONAZITE U-PB DATING AND ^{40}AR-^{39}AR THERMOCHRONOLOGY OF METAMORPHIC EVENTS IN THE CENTRAL AFRICAN COPPERBELT DURING THE PAN-AFRICAN LUFILIAN OROGENY

ABSTRACT

New SHRIMP U-Pb age data on metamorphic monazite, as well as step-heating ^{40}Ar-^{39}Ar ages on metamorphic biotite, muscovite and microcline, from Katangan metasedimentary rocks of the Central African Copperbelt are presented. These rocks were deformed and metamorphosed during the Pan-African Lufilian Orogeny. Three samples of metamorphic monazite from the Chambishi structural basin give ages of 592 ± 22 Ma, 531 ± 12 Ma and 512 ± 17 Ma, which correspond respectively to the ages of eclogite facies metamorphism, high pressure talc-kyanite whiteschist metamorphism, and of a regional metamorphism/ mineralisation pulse elsewhere within the Lufilian Orogen. A biotite population from Luanshya gives a ^{40}Ar/^{39}Ar plateau age of 586.1 ± 1.7 Ma, coinciding with the oldest monazite age. Several samples from the Chambishi basin and the Konkola area give ^{40}Ar/^{39}Ar biotite plateau ages in the range of 496.6 ± 0.6 to 485.2 ± 0.9 Ma, and a muscovite plateau age of 483.6 ± 1.1 Ma, which are a manifestation of regional uplift and cooling that affected the whole Katangan basin. The youngest apparent ^{40}Ar/^{39}Ar ages obtained are from microcline at Musoshi and range from 467.0 ± 2.7 Ma to 405.8 ± 3.8 Ma, reflecting continued slow cooling of the Lufilian Orogen.

_____oOo_____

MONAZITE U-PB DATING AND ^{40}AR-^{39}AR THERMOCHRONOLOGY OF METAMORPHIC EVENTS IN THE CENTRAL AFRICAN COPPERBELT DURING THE PAN-AFRICAN LUFILIAN OROGENY

CONTENTS

	Page
INTRODUCTION	1
REGIONAL SETTING	1
ANALYTICAL METHODS	1
SAMPLING	2
RESULTS	4
Muliashi South deposit (Luanshya), sample BH89/3,biotite	4
Chambisi basin, sample RCB2/72, monazite	6
Chambisi basin, sample NN75/26, biotite	6
Chambisi basin, sample RCB1/36, monazite	7
Chambisi basin, sample RCB2/112, monazite	7
Chambisi basin, sample RCB2/112, biotite	11
Chambisi basin, sample RCB2/4, biotite	12
Chambisi basin, sample MJZC9/25, biotite	12
Chambisi basin, sample NN75/9, biotite	12
Nchanga, sample NCH1, biotite	15
Konkola, sample KN1A, biotite and muscovite	17
Musoshi (DRC), sample MUS 1, microcline	20
DISCUSSION	20
Geochronology	21
Regional implications	23
ACKNOWLEDGEMENTS	24
REFERENCES	24

oOo

Published by the Economic Geology Research Institute
School of Geosciences
University of the Witwatersrand
1 Jan Smuts Avenue
Johannesburg
South Africa
http://www.wits.ac.za/geosciences/egri.htm
ISBN 0-9584855-8-5

INFORMATION CIRCULAR No. 391

(for Restricted Distribution)

MONAZITE U-PB DATING AND ^{40}AR-^{39}AR THERMOCHRONOLOGY OF METAMORPHIC EVENTS IN THE CENTRAL AFRICAN COPPERBELT DURING THE PAN-AFRICAN LUFILIAN OROGENY

INTRODUCTION

This paper is part of a wider geochronological study of the Central African Copperbelt and its basement. After constraining the nature and evolution of the basement of the Copperbelt (Rainaud *et al*. 2003, 2005), and the provenance of key units within the Katanga Supergroup and their ages (Master *et al*., 2005), in this paper we provide new data dealing with the several metamorphic episodes which occurred in the Central African Copperbelt during the Lufilian Orogeny, and discuss their implications for the evolution of the Katangan basin

REGIONAL SETTING

The Katanga Supergroup is the host of the major stratiform sediment-hosted Cu-Co deposits, as well as numerous other deposits of Cu, Pb, Zn, U, Au, Fe et*c.*, which constitute the Central African Copperbelt in Zambia and the Democratic Republic of Congo. This succession is a Neoproterozoic metasedimentary sequence which consists of the Roan Group, the Nguba Group, the Fungurume and the Biano Groups (Wendorff, 2001a,b; 2002a,b; 2003a,b; Cailteux, 2003). The lowermost Roan Group was deposited after *c.* 880 Ma (Armstrong *et al*., 1999), and is subdivided into the mainly siliciclastic Lower Roan Subgroup, and the mainly dolomitic and evaporitic Upper Roan Subgroup (Master *et al*., 2005). The base of the Nguba Group, the Mwashya Subgroup, was deposited at around 765 Ma (Key *et al*., 2001), while porphyritic lavas attributed to the upper part of the Nguba Group were dated at 735 Ma (Armstrong, 2000; Liyungu *et al*., 2001; Key *et al*., 2001). The Mwashya Subgroup is overlain by the Grand Conglomerat Member, which is a glacial tillite (Master *et al*., 2005). Finally, the Fungurume and Biano Groups were deposited syntectonically in a foreland basin during the Lufilian Orogeny, after *c.* 572 Ma (Wendorff, 2003a; Master *et al*., 2005).

The Katanga Supergroup was deformed and metamorphosed during the Pan-African Zambezi and Lufilian orogenies (Porada and Berhorst, 2000), at between 600 and 480 Ma. Metamorphism in the Zambian Copperbelt was mainly of greenschist facies, except at Muliashi, where epidote-amphibolite facies assemblages were recognised, characterised by the presence of tremolite, biotite, epidote and actinolite in impure dolomites, and of scapolite and clinozoisite in argillites (Mendelsohn, 1961). In the Domes area to the west of the Copperbelt, amphibolite facies assemblages are recognised (Cosi *et al*., 1992). A large number of imprecise U-Pb, Rb-Sr and K-Ar age data from the Lufilian Arc and Zambezi Belt, spanning the time period 500 ± 100 Ma are summarised by Cahen *et al*. (1984). More recently, the Kipushi deposit was dated at 454 Ma (Walraven and Chabu, 1994) but was also recalculated at 750 Ma using a three-stage model (Kampunzu *et al*., 1998). In the Musoshi district, U-Pb analyses on uraninite and rutile yielded ages of *c.* 514 Ma (Richards *et al*., 1988a, b). Molybdenite from Kansanshi (Zambia) yielded ages of *c.* 512 and 502 Ma with the Re-Os technique (Torrealday *et al*., 2000). Eclogites from Central Zambia yielded a Sm-Nd isochron at 595 ± 10 Ma (John *et al*., 2003) while a phase of high-pressure whiteschist metamorphism yielded a U-Pb monazite age of 529 ± 2 Ma (John *et al*., 2004).

ANALYTICAL METHODS

^{40}Ar-^{39}Ar analyses were performed at the Research School of Earth Sciences (RSES), Australian National University, Canberra. Muscovites were separated at the the Hugh Allsopp Laboratory,

University of the Witwatersrand, Johannesburg, South Africa. Samples were reduced in a jaw crusher and through a pulverizer into a coarse powder which was then sieved. Extracts were purified at the Australian National University, using conventional magnetic separation and heavy liquid techniques. The resulting separates were of ~99% or higher purity. The $^{40}Ar/^{39}Ar$ dating technique used was described in detail by McDougall and Harrison (1999). Crystals were placed into an aluminium irradiation canister together with interspersed aliquots of the flux monitor GA 1550 (age = 98.5 Ma; Spell and McDougall, 2003). Packets containing degassed potassium glass were placed at either end of the canister to monitor the ^{40}Ar production from potassium (e.g. Tetley, 1980). The irradiation canister was irradiated for 504 hours in position X34 of the ANSTO, HIFAR reactor, Lucas Heights, New South Wales, Australia. The canister, which was lined with 0.2 mm Cd to absorb thermal neutrons, was inverted three times during the irradiation, which reduced neutron flux gradients to < 2% along the length of the canister. Mass discrimination was monitored by analyses of standard air volumes. Correction factors for interfering reactions are as follows: $(^{40}Ar/^{39}Ar)_{Ca} = 3.50(\pm 0.14)x10^{-4}$; $(^{39}Ar/^{37}Ar)_{Ca} = 7.86(\pm 0.01)x10^{-4}$ (McDougall and Harrison, 1999); $(^{40}Ar/^{39}Ar)_{K} = 0.050 (\pm 0.005)$. K/Ca ratios were determined from the ANU laboratory hornblende standard 77-600 and were calculated as follows: $K/Ca = 1.9 \times {}^{39}Ar/^{37}Ar$. The reported data have been corrected for system blanks, mass discrimination and radioactive decay. The calculated ages have been corrected additionally for reactor interferences, fluence gradients and atmospheric contamination. Errors associated with the age determinations are one sigma uncertainties and include errors in the J-value estimates. The error on the J-value is ± 0.35 %, excluding the uncertainty in the age of GA1550 (which is ~ 1%). Decay constants are those of Steiger and Jäger (1977).

Plateau portions of the age spectra are defined as comprising at least three contiguous increments, with concordant ages (i.e. ages that are within two sigma of the mean age). In addition, this segment should contain a significant proportion of the total ^{39}Ar released (MacDougall, 1999).

U-Pb analyses were performed on the SHRIMP II ion microprobe at the Australian National University, Canberra. The separation of monazites was carried out at the Hugh Allsopp Laboratory, Johannesburg, using a Wilfley Table, a Frantz Isodynamic Magnetic Separator, and heavy liquids. The SHRIMP analytical procedure used in this study is similar to that described by Claoué-Long *et al*. (1995). Age calculations and plotting were done using Isoplot/Ex (Ludwig, 2000).

SAMPLING

Eleven samples were utilised for the purpose of this study (Fig. 1): seven were located in the Chambishi basin in Zambia (Fig. 2), one in the Konkola area (also in Zambia), one in the Muliashi South deposit (Zambia, near Luanshya), one in the Nchanga mine (Zambia) and finally, one in the Musoshi Mine in the Democratic Republic of Congo (Fig. 1). Two of these samples were dated by two methods.

In one sample (sample RCB2/112), monazites were extracted and dated with the SHRIMP U-Pb technique while a population of biotite crystals was analysed with the ^{40}Ar-^{39}Ar technique. With the sample KN1A (from the Konkola area) muscovite and biotite crystal populations were dated with the ^{40}Ar-^{39}Ar dating technique. Monazites from three samples collected in the Chambishi basin were analysed using the SHRIMP U-Pb technique. Biotite from six samples and microclines from one sample were analysed using the ^{40}Ar-^{39}Ar technique. All samples are derived from the Lower Roan Subgroup up to the Grand Conglomerat Formation (Fig. 3).

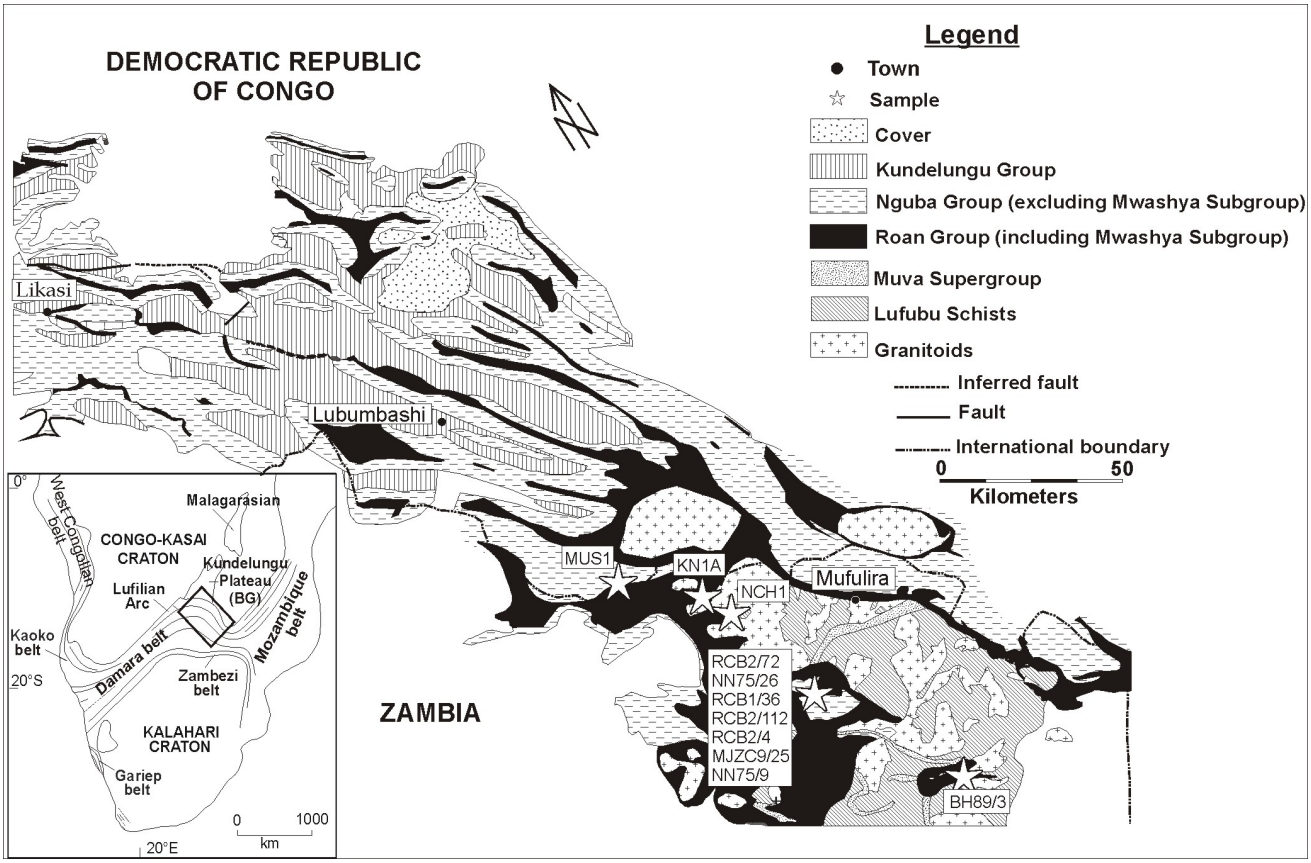

Figure 1. *Simplified geological map of the Copperbelt and location of samples (after François, 1974).*

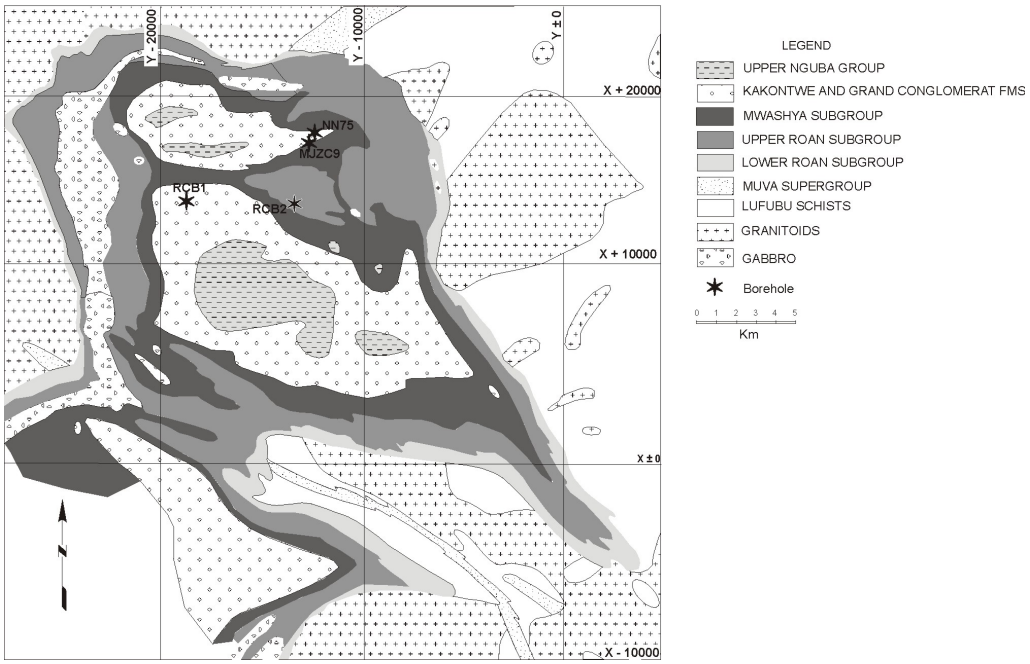

Figure 2. *Simplified geological map of the Chambishi basin and location of drill holes (after JICA/MMAJ, 1996).*

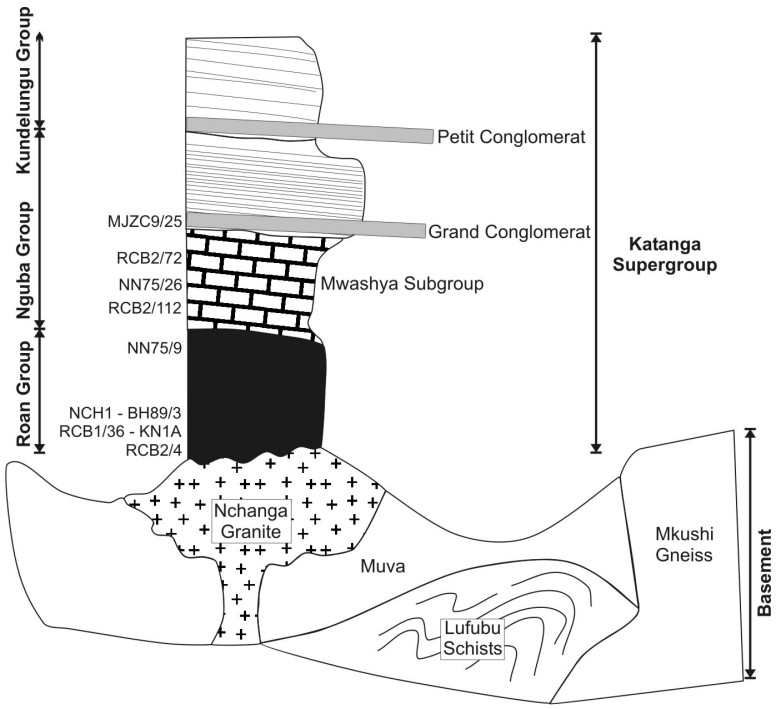

Figure 3

Figure 3. *Stratigraphic position of the samples*

RESULTS

Samples analysed and dated in this study yielded several distinct age ranges. Three samples give an age range between 631.8 ± 1.8 Ma and 586.1 ± 1.7 Ma, 6 samples give an age range between 496.6 ± 0.6 Ma and 467.0 ± 2.7 Ma while individual samples give ages of 531 ± 12 Ma and 512 ± 17 Ma.

Muliashi South deposit (Luanshya), sample BH89/3, biotite

Borehole BH89 is located on the southern flank of the Roan Antelope synclinorium and more precisely on the Muliashi South deposit (Fig. 1) where reserves are estimated at 22 Mt grading at 2.32% Cu (Mbendi, 2002). This bore hole is 975.36 m deep and reaches the pre-Katangan basement. Sample BH89/3 is located 743 m below the surface and at 35 m above the contact between the sedimentary sequence and the pre-Katangan basement. Stratigraphically, the sample is situated within the Ore Shale Formation at the base of the Upper Roan Subgroup. It is a biotite-tremolite-quartz schist with a porphyroblastic texture which also contains bornite and chalcopyrite. Retrograde metamorphism is reflected by biotite being replaced by chlorite. Step-heating ^{40}Ar-^{39}Ar was undertaken on a 0.47 mg population of biotite. Data are reported in a diagram of age versus %^{39}Ar released (Fig. 4 and Table 1). The first apparent age, connected to a degassing temperature of 600ºC, is 469.5 ± 6.7 Ma and corresponds to 0.934% of the ^{39}Ar released. The diagram presents two peaks at the temperatures 680ºC and 850ºC with apparent ages at 602.5 ± 2.8 Ma and 602.2 ± 2.3 Ma respectively. Between these older apparent ages and for 55.52% of the ^{39}Ar released (equivalent to 5 consecutive increments), the apparent ages vary between 583.3 ± 1.8 Ma and 588.7 ± 1.5 Ma and yield a plateau age at 586.1 ± 1.7 Ma with a MSWD at 1.4. The steps following the second peak, at 950ºC and 1050ºC show similar ages

Table 1. ^{40}Ar-^{39}Ar step-heating analytical results, sample BH89/3 biotite

Temp (C)	Cum $^{\%39}Ar$	$^{40}Ar/^{39}Ar$	$^{37}Ar/^{39}Ar$	$^{36}Ar/^{39}Ar$	Vol. ^{39}Ar x10^{-15}mol	%Rad. ^{40}Ar	Ca/K	$^{40}Ar^*/^{39}Ar$	Age (Ma)	± 1σ.d. (Ma)
Mass = 0.47 mg										
J-value = 0.010224 ± 0.000025										
600	0.97	39.22	0.0163	0.0342	0.859	74.1	0.0311	29.07	469.5	6.7
680	3.07	42.45	0.0007	0.0122	1.868	91.4	0.0014	38.78	602.5	2.8
720	11.47	38.68	0.0000	0.0035	7.451	97.1	0.0001	37.58	586.6	2.0
740	23.88	38.07	0.0000	0.0010	11.02	99.1	0.0000	37.74	588.7	1.5
760	37.77	37.83	0.0000	0.0015	12.33	98.6	0.0000	37.34	583.3	1.8
780	50.26	37.73	0.0001	0.0006	11.08	99.3	0.0001	37.47	585.2	1.9
800	58.59	38.04	0.0000	0.0015	7.397	98.7	0.0001	37.54	586.0	2.7
850	65.23	39.11	0.0001	0.0010	5.886	99.1	0.0002	38.76	602.2	2.3
950	85.30	38.56	0.0002	0.0006	17.81	99.4	0.0004	38.32	596.4	1.8
1050	99.61	38.70	0.0000	0.0012	12.70	98.9	0.0000	38.28	595.9	1.9
1150	99.96	52.03	0.0339	0.0515	0.314	70.6	0.0645	36.75	575.5	19.1
1300	100.0	230.12	0.2652	0.8582	0.033	-10.2	0.5040	0.00	0.0	0.0
Total		37.17	0.0252	0.0012	88.74			37.80	589.5	2.2

I) Errors are one sigma uncertainties and exclude uncertainties in the J-value.
ii) Data are corrected for mass spectrometer backgrounds, discrimination and radioactive decay.
iii) Interference corrections: $(^{36}Ar/^{37}Ar)_{Ca}$ = 3.49E-4; $(^{39}Ar/^{37}Ar)_{Ca}$ = 7.86E-4; $(^{40}Ar/^{39}Ar)_{K}$ = 0.042
iv) J-values are based on an age of 97.9 Ma for GA-1550 biotite.

at 596.4 ± 1.8 Ma and 595.9 ± 1.9 Ma. Finally, the step at 1150ºC yielded an apparent age of 575.5 ± 19.1 Ma.

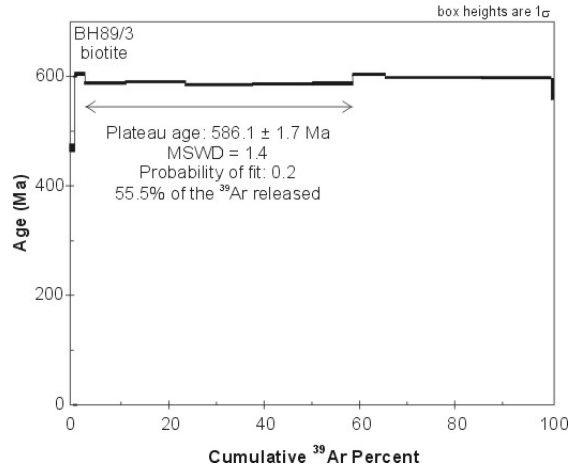

Figure 4. *Age vs. ^{39}Ar released diagram, sample BH89/3*

Chambishi basin, sample RCB2/72, monazite

Borehole RCB2 is 1840.68 m long and is located at the western limit of the Chambishi Southeast prospect (Fig. 2). It reaches the basal conglomerate of the Katangan sedimentary sequence. This sample was collected at a depth of 497 m and is stratigraphically situated in the Mwashya Subgroup. Sample RCB2/72 is from an iron formation interbedded with an altered tuff (biotite retrograded to chlorite, quartz and carbonate). Monazites are anhedral and green, intergrown with biotite or chlorite and clearly of metamorphic origin. Metamorphic monazites were analysed using the U-Pb SHRIMP technique. Data are reported in a Tera-Wasserburg diagram, Figure 5 and in Table 2. Analyses plot on a discordia intercepting the concordia curve. The weighted mean $^{206}Pb/^{238}U$ age is 592 ± 22 Ma, which is interpreted as the age of formation of these monazites.

Table 2. SHRIMP Th-U-Pb results from monazites, sample RCB2/72

						Measured Ratios				Apparent Ages (Ma)			
Grain. spot	U (ppm)	Th (ppm)	Th/U	Pb* (ppm)	f_{206} %	$^{208}Pb/^{238}U$	±	$^{206}Pb/^{238}U$	±	$^{208}Pb/^{238}U$	±	$^{206}Pb/^{238}U$	±
1.1	167	6380	38.2	180	2.31	0.0299	0.0035	0.0934	0.0093	596	68	575	55
2.1	178	8676	48.8	245	2.13	0.0304	0.0035	0.0993	0.0096	604	70	610	57
3.1	204	7301	35.8	266	2.00	0.0388	0.0045	0.1084	0.0103	770	87	664	60
4.1	223	6832	30.7	207	1.32	0.0317	0.0034	0.0933	0.0083	630	66	575	49
5.1	193	9422	48.9	293	1.87	0.0337	0.0036	0.0976	0.0090	670	71	600	53
6.1	220	6847	31.1	209	1.75	0.0320	0.0040	0.0959	0.0101	637	78	590	60
7.1	261	18329	70.3	436	1.20	0.0261	0.0024	0.0910	0.0071	520	47	561	42
8.1	178	6465	36.3	170	1.22	0.0278	0.0024	0.0870	0.0065	554	47	538	38
9.1	161	5571	34.5	151	0.41	0.0285	0.0038	0.0879	0.0100	569	75	543	59
10.1	183	9814	53.6	261	0.15	0.0288	0.0022	0.0968	0.0062	574	43	595	36
11.1	207	4613	22.3	153	0.51	0.0335	0.0030	0.0994	0.0073	666	59	611	43
12.1	288	5824	20.2	188	0.07	0.0319	0.0021	0.0998	0.0056	635	41	613	33
13.1	209	5566	26.7	181	0.75	0.0336	0.0027	0.0974	0.0065	668	53	599	38
14.1	197	10148	51.6	274	0.06	0.0292	0.0026	0.0959	0.0075	582	52	590	44
15.1	181	4330	23.9	137	0.88	0.0322	0.0023	0.0990	0.0060	641	45	608	35

Notes : (1) Uncertainties given at the one σ level; (2) f206 % denotes the percentage of ^{206}Pb that is common Pb.

Chambishi basin, sample NN75/26, biotite

Borehole NN75 is located in the northeast area of the Chambishi basin, designated as the Southeast prospect (Fig. 2). It is 1033.78 m long, and penetrates the Katanga Supergroup to reach a granite that forms, together with the Lufubu schists, the local pre-Katangan basement (Rainaud *et al*., 2005). The sample NN75/26 was collected at a depth of 148 m, in a magnetite-rich iron-formation located 2 m below a tuffaceous layer in the Mwashya Subgroup. Between the grains of iron oxides, intergrowths of chlorite - biotite, calcite and quartz are developed. A population of biotite crystals, weighing 1.00 mg

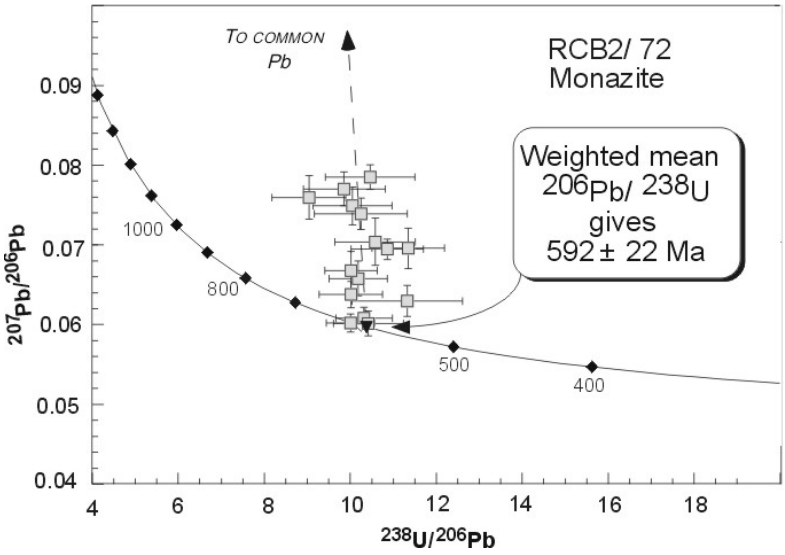

Figure 5. *Tera-Wasserburg diagram, sample RCB2/72*

was analysed by the ^{40}Ar-^{39}Ar technique. Data are reported in a diagram of age versus %^{39}Ar released (Fig. 6; Table 3). This diagram presents a hump-shaped ^{40}Ar-^{39}Ar age profile. Apparent ages vary between 53.7 ± 1.0 Ma and 631.8 ± 1.8 Ma for temperatures between 650ºC and 970º*C*. For temperatures between 1000ºC and 1100ºC, apparent ages vary between 614.7 ± 1.8 Ma and 554.4 ± 3.1 Ma. No plateau age can be extracted and apparent ages are greater than the ones previously yielded by other samples.

Chambishi basin, sample RCB1/36, monazite

Borehole RCB1 is located 5 km west of RCB2 (Fig. 2) and is 1686.2 m deep. RCB1/36 was sampled at 1284 m and is stratigraphically located in the Upper Roan Subgroup. This sample is a metapelite including biotite, quartz and K-feldspar. As seen previously in sample RCB272, monazites are green, anhedral and clearly metamorphi*c.* They were extracted and analysed with the SHRIMP U-Pb technique. Results are reported in Table 4 and presented in a Tera-Wasserburg concordia diagram in Figure 7. Plots are clustered near the concordia and the weighted mean yields a ^{206}Pb/^{238}U age of 531 ± 12 Ma. This age is interpreted as the age of formation of the monazites.

Chambishi basin, sample RCB2/112, monazite

Sample RCB2/112 was taken at a depth of 528 m, in the borehole RCB2. This sample is a marly dolomitic argillite from the Mwashya Subgroup. Monazites were analysed with the U-Pb SHRIMP dating technique. Data are reported in a Tera-Wasserburg concordia diagram (Fig. 8; Table 5). Analyses plot in a cluster and yield weighted mean ^{206}Pb/^{238}U at 512 ± 17 Ma. This age is interpreted as the age of formation of these monazites.

Table 3. Data ^{40}Ar-^{39}Ar, sample NN75/26 biotite

Temp (C)	Cum $^{\%39}Ar$	$^{40}Ar/^{39}Ar$	$^{37}Ar/^{39}Ar$	$^{36}Ar/^{39}Ar$	Vol. ^{39}Ar $x10^{-15}$mol	%Rad. ^{40}Ar	Ca/K	$^{40}Ar^*/^{39}Ar$	Age (Ma)	± 1σ.d. (Ma)
Mass = 1.00 mg										
J-value = 0.010209 ± 0.000025										
650	11.36	8.55	0.1223	0.0188	42.73	34.6	0.2320	2.96	53.7	1.0
700	13.23	28.33	0.2466	0.0145	7.039	84.8	0.4690	24.04	395.9	3.8
740	16.13	35.16	0.0080	0.0121	10.94	89.7	0.0153	31.54	503.6	3.5
780	18.60	34.69	0.0153	0.0103	9.30	91.1	0.0290	31.58	504.1	3.3
820	23.08	34.12	0.0105	0.0076	16.84	93.3	0.0200	31.84	507.7	1.9
850	28.57	37.80	0.0047	0.0052	20.64	95.8	0.0090	36.23	567.8	1.6
870	35.08	38.84	0.0273	0.0052	24.50	95.9	0.0518	37.25	581.4	3.2
890	40.79	39.82	0.0062	0.0033	21.50	97.5	0.0119	38.80	602.0	1.5
910	47.12	40.58	0.0059	0.0029	23.82	97.8	0.0112	39.70	613.8	2.7
940	56.86	41.49	0.0061	0.0019	36.66	98.5	0.0116	40.88	629.2	1.8
970	70.36	41.67	0.0050	0.0018	50.78	98.6	0.0095	41.08	631.8	1.8
1000	84.49	40.32	0.0028	0.0017	53.17	98.6	0.0054	39.77	614.7	1.8
1050	98.42	37.38	0.0016	0.0023	52.43	98	0.0031	36.65	573.4	1.5
1100	99.96	39.74	0.0168	0.0151	5.803	88.7	0.0319	35.24	554.4	3.1
1150	99.99	253.70	1.5573	0.6235	0.113	27.4	2.9600	69.67	969.2	350.3
1200	100.0	1136.78	56.5702	4.2273	0.024	-9.4	112.00	0.00	0.0	3296
Total		35.69	0.0286	0.0060	376.3			33.87	535.7	2.2

I) Errors are one sigma uncertainties and exclude uncertainties in the J-value.

ii) Data are corrected for mass spectrometer backgrounds, discrimination and radioactive decay.

iii) Interference corrections: $(^{36}Ar/^{37}Ar)_{Ca}$ = 3.49E-4; $(^{39}Ar/^{37}Ar)_{Ca}$ = 7.86E-4; $(^{40}Ar/^{39}Ar)_{K}$ = 0.042

iv) J-values are based on an age of 97.9 Ma for GA-1550 biotite.

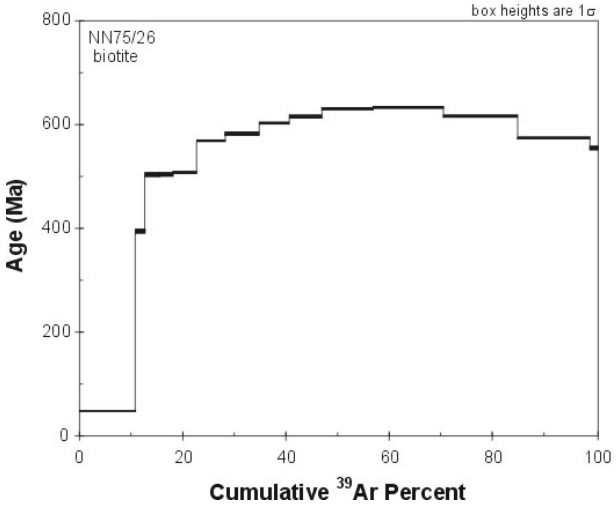

Figure 6. *Age vs. ^{39}Ar released diagram, sample NN75/26*

Table 4. SHRIMP Th-U-Pb results from monazites, sample RCB1/36

						Measured Ratios				Apparent Ages (Ma)			
Grain. spot	U (ppm)	Th (ppm)	Th/U	Pb* (ppm)	f_{206} %	$^{208}Pb/^{238}U$	±	$^{206}Pb/^{238}U$	±	$^{208}Pb/^{238}U$	±	$^{206}Pb/^{238}U$	±
1.1	651.2	4991.4	7.7	166	0.28	0.02647	0.00172	0.08659	0.0048	528	34	535	29
2.1	1002	1151	1.1	111	0.78	0.0275	0.0018	0.0916	0.0050	549	36	565	29
3.1	621	2939	4.7	116	0.76	0.0264	0.0024	0.0869	0.0068	527	48	537	41
4.1	716	5573	7.8	185	0.14	0.0263	0.0011	0.0891	0.0035	524	22	550	20
5.1	654	4382	6.7	151	0.56	0.0260	0.0012	0.0875	0.0037	519	25	541	22
6.1	633	4157	6.6	145	0.52	0.0263	0.0012	0.0874	0.0036	524	24	540	21
7.1	629	2991	4.8	110	0.40	0.0246	0.0013	0.0811	0.0038	491	25	503	22
8.1	763	4546	6.0	160	0.31	0.0256	0.0015	0.0848	0.0044	511	30	525	26
9.1	787	4481	5.7	159	0.31	0.0253	0.0013	0.0842	0.0039	505	26	521	23
10.1	768	4393	5.7	159	0.19	0.0257	0.0011	0.0866	0.0034	514	22	536	20
11.1	848	4629	5.5	172	0.15	0.0262	0.0012	0.0871	0.0035	523	23	538	21
12.1	882	4129	4.7	155	0.39	0.0250	0.0017	0.0815	0.0047	498	33	505	28
13.1	596	2549	4.3	100	0.79	0.0248	0.0017	0.0832	0.0048	495	33	515	29
14.1	740	3777	5.1	134	0.35	0.0246	0.0015	0.0803	0.0043	490	29	498	26
15.1	373	5291	14.2	151	0.65	0.0264	0.0016	0.0892	0.0045	527	31	551	27

Notes : (1) Uncertainties given at the one σ level; (2) f206 % denotes the percentage of ^{206}Pb that is common Pb.

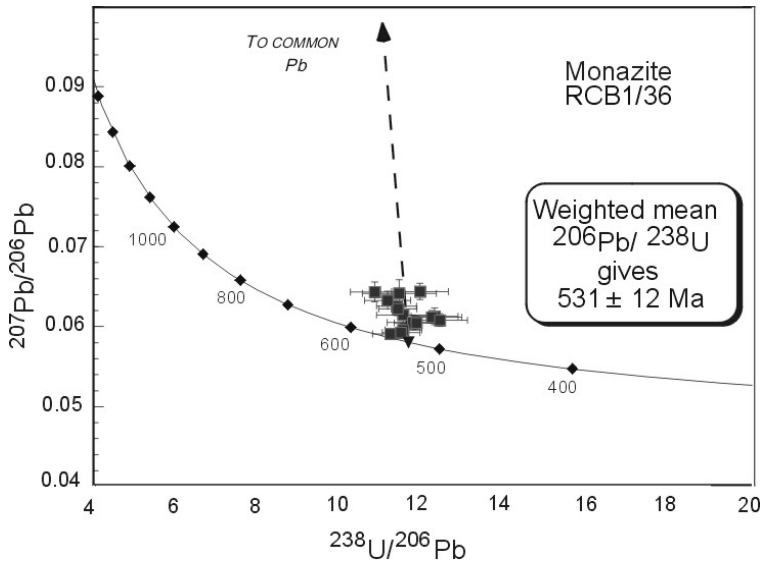

Figure 7. *Tera-Wasserburg diagram, sample RCB1/36*

Table 5. SHRIMP Th-U-Pb results from monazites, sample RCB2/112

Grain. spot	U (ppm)	Th (ppm)	Th/U	Pb* (ppm)	f_{206} %	Measured Ratios				Apparent Ages (Ma)			
						$^{208}Pb/^{238}U$	±	$^{206}Pb/^{238}U$	±	$^{208}Pb/^{238}U$	±	$^{206}Pb/^{238}U$	±
1.1	195	24945	127.9	531	0.53	0.0238	0.0019	0.0829	0.0057	476	37	513	34
2.1	140	12888	92.0	304	0.97	0.0262	0.0020	0.0877	0.0057	523	39	542	34
3.1	164	19244	117.1	423	0.38	0.0246	0.0021	0.0841	0.0061	491	41	520	37
4.1	169	20307	119.9	423	0.59	0.0233	0.0023	0.0781	0.0065	466	45	485	39
5.1	204	25790	126.4	531	0.58	0.0231	0.0016	0.0763	0.0046	462	31	474	27
6.1	193	18817	97.3	449	0.39	0.0266	0.0024	0.0898	0.0068	530	46	554	41
7.1	173	15684	90.7	359	1.25	0.0254	0.0020	0.0836	0.0058	508	40	518	34
8.1	177	22893	129.4	497	0.52	0.0244	0.0020	0.0824	0.0058	487	39	510	34
9.1	170	21718	127.7	493	0.73	0.0255	0.0019	0.0860	0.0055	508	37	532	32
10.1	136	10044	73.7	224	0.91	0.0246	0.0019	0.0802	0.0055	491	38	497	33
11.1	187	23817	127.5	511	0.80	0.0241	0.0017	0.0799	0.0049	481	34	496	29
12.1	198	24235	122.2	538	0.63	0.0249	0.0016	0.0853	0.0046	497	31	528	28
13.1	222	27096	122.3	554	0.30	0.0229	0.0027	0.0773	0.0080	457	54	480	48
14.1	200	24376	122.0	559	0.53	0.0257	0.0019	0.0871	0.0057	513	38	538	34
15.1	179	14724	82.3	325	0.66	0.0244	0.0016	0.0820	0.0047	488	32	508	28

Notes : (1) Uncertainties given at the one σ level; (2) f206 % denotes the percentage of ^{206}Pb that is common Pb.

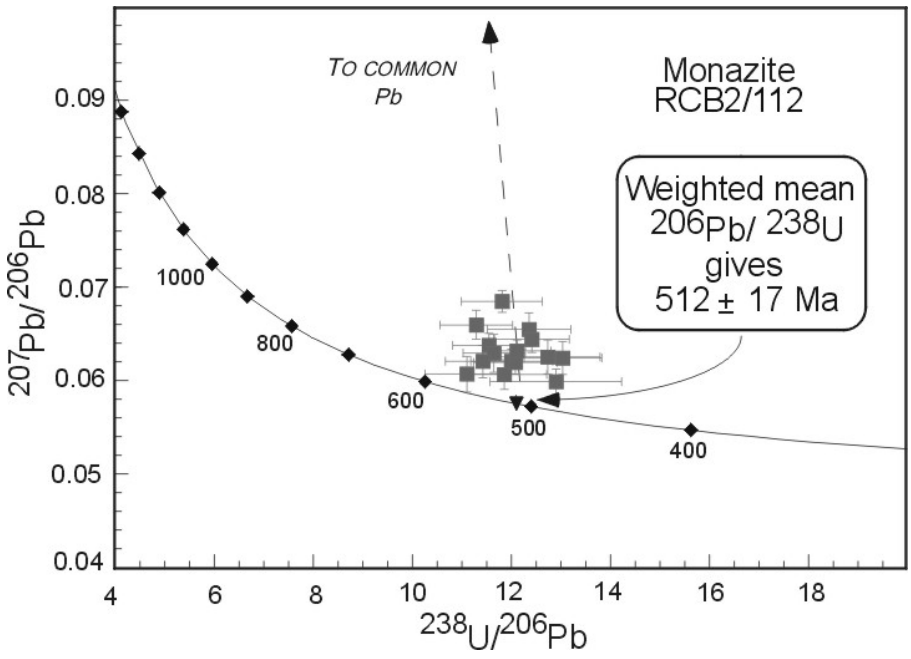

Figure 8. *Tera-Wasserburg diagram, sample RCB2/112*

Chambishi basin, sample RCB2/112, biotite

After obtaining the U-Pb SHRIMP age data on monazites (see above), a population of biotite grains weighing 0.83 mg was separated. The biotite grains were dated with the ^{40}Ar-^{39}Ar technique and the results are reported in Table 6 and the age data plotted in Figure 9. The first step at 650ºC yields a very young apparent age at 307.2 ± 2.6 Ma. The next two steps at 700ºC and 740ºC produce older ages of 458.3 ± 1.8 Ma and 486.1 ± 1.5 Ma. The next seven steps, with temperatures between 760ºC and 940ºC, yield apparent ages between 488.5 ± 1.5 Ma and 494.7 ±1.8 Ma. The extracted plateau age of this section is of 491.5 ± 1.6 Ma, with a MSWD = 1.7, and corresponds to 66.4% of the ^{39}Ar released. The last section of the spectrum yields two older apparent ages (at 496.0 ± 1.2 Ma and 497.7 ± 1.4 Ma) and finally a much younger apparent age at 456.3 ± 8.1 Ma.

Table 6. Data ^{40}Ar-^{39}Ar, sample RCB2/112 biotite

Temp (C)	Cum $^{\%39}Ar$	$^{40}Ar/^{39}Ar$	$^{37}Ar/^{39}Ar$	$^{36}Ar/^{39}Ar$	Vol. ^{39}Ar x10^{-15}mol	%Rad. ^{40}Ar	Ca/K	$^{40}Ar^*/^{39}Ar$	Age (Ma)	± 1σ.d. (Ma)
Mass = 0.83 mg										
J-value = 0.010193 ± 0.000025										
650	1.87	26.51	0.2602	0.0280	2.889	68.7	0.4950	18.21	307.2	2.6
700	5.97	33.45	0.1619	0.0170	6.355	84.8	0.3080	28.38	458.3	1.8
740	16.21	31.69	0.0158	0.0044	15.86	95.7	0.0300	30.34	486.1	1.5
760	28.05	31.17	0.0007	0.0015	1.833	98.4	0.0013	30.66	490.7	1.4
780	41.08	30.96	0.0001	0.0013	20.16	98.6	0.0002	30.51	488.5	1.5
800	53.44	31.07	0.0008	0.0011	19.14	98.8	0.0015	30.68	490.9	1.0
820	63.61	30.97	0.0000	0.0006	15.75	99.2	0.0000	30.74	491.7	1.9
840	69.84	31.29	0.0005	0.0017	9.641	98.2	0.0010	30.74	491.8	1.4
870	73.51	31.74	0.0022	0.0025	5.690	97.5	0.0041	30.95	494.7	1.8
940	82.64	31.39	0.0121	0.0016	14.13	98.3	0.0230	30.85	493.3	1.2
1020	95.33	31.54	0.0015	0.0015	19.66	98.4	0.0029	31.05	496.0	1.2
1060	99.65	32.08	0.0083	0.0028	6.678	97.2	0.0158	31.17	497.7	1.4
1300	100.0	45.48	0.1210	0.0582	0.549	62.1	0.2300	28.23	456.3	8.1
Total		31.36	0.0155	0.0031	154.80			30.39	486.8	1.5

I) Errors are one sigma uncertainties and exclude uncertainties in the J-value.
ii) Data are corrected for mass spectrometer backgrounds, discrimination and radioactive decay.
iii) Interference corrections: $(^{36}Ar/^{37}Ar)_{Ca}$ = 3.49E-4; $(^{39}Ar/^{37}Ar)_{Ca}$ = 7.86E-4; $(^{40}Ar/^{39}Ar)_{K}$ = 0.042
iv) J-values are based on an age of 97.9 Ma for GA-1550 biotite.

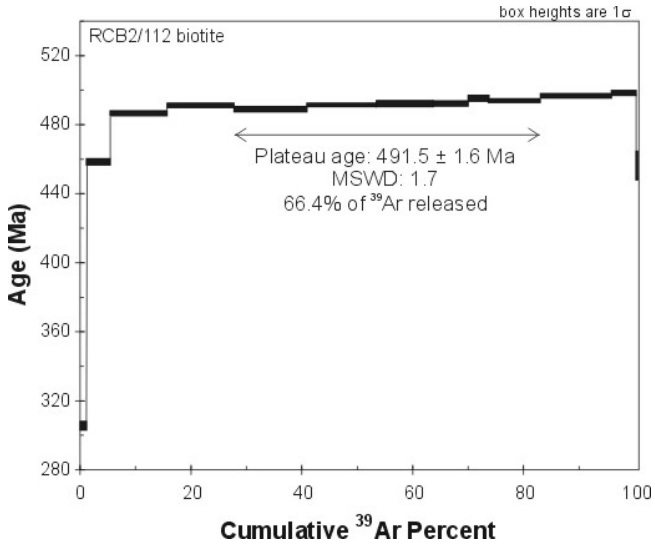

Figure 9. *Age vs. ^{39}Ar released diagram, sample RCB2/112*

Chambishi basin, sample RCB2/4, biotite

This sample is from the Lower Roan Subgroup and was collected at a depth of 1468 m from borehole RCB2. It is from a 0.5m thick biotite-bearing trough-crossbedded sandstone interbedded with conglomerates of the basal Roan Group. A population of biotite grains from this sample was analysed and the results are reported in Table 7, and plotted in Figure 10. The two first steps, at 650 ºC and 700ºC, present apparent ages at 468.3 ± 3.6 Ma and 484.9 ± 1.6 Ma respectively. The following seven steps, for temperatures between 720ºC and 800 ºC, yield apparent ages ranging from 488.8 ± 1.7 Ma to 493.4 ± 1.7 Ma. These seven apparent ages yield a plateau age at 490.9 ± 0.6 Ma with a MSWD = 1.2 and with 75% of the ^{39}Ar released. The following step at 850ºC presents a peak in the apparent ages at 495.2 ± 1.8 Ma. The last three steps at 900, 1000 and 1200ºC yield apparent ages at, respectively, 482.6 ± 2.9 Ma, 488.7 ± 2.0 Ma and 481.7 ± 5.3 Ma.

Chambishi basin, sample MJZC9/25, biotite

Borehole MJZC9 is located in the Chambishi basin, less than 1 km southwest of the borehole NN75 (Figs. 1 and 2). This borehole is 1140 m deep and the sample MJZC9/25 came from a depth of 152 m. The sample is a laminated grey shale located in the Grand Conglomerat Formation, and comprises mainly quartz, sericite and biotite. A population of biotite crystals weighing 0.3 mg was separated and analysed with the ^{40}Ar-^{39}Ar technique. Results of analyses are reported in Table 8 and in an age spectrum (Fig. 11). The first two steps at 650ºC and 740ºC yield apparent ages at 393.1 ± 6.0 Ma and 481.0 ± 1.3 Ma. The following five steps, between 760ºC and 880ºC, yield apparent ages ranging between 487.3 ± 4.1 and 483.0 ± 1.9 Ma and a plateau age at 485.2 Ma ± 0.9 Ma (with a MSWD at 0.7) which corresponds to 62.4 % of the ^{39}Ar released. The last part of the spectrum, from 950ºC to 1100ºC, presents a convex shape with a peak of apparent age at 490.8 ± 1.8 Ma (at 950ºC).

Chambishi basin, sample NN75/9, biotite

Sample NN75/9 was taken at a depth of 893.6 m in borehole NN75, in the Chambishi Basin. It is located in the hangingwall of the orebody, in the Ore Shale Formation of the Upper Roan Subgroup. This sample is a rippled white dolarenite with specks of metamorphic biotite. A population of biotite

Table 7. Data ^{40}Ar-^{39}Ar, sample RCB2/4 biotite

Temp (C)	Cum $^{\%39}Ar$	Vol. ^{39}Ar x10^{-14}mol	K/Ca	% Ar39 rel	$^{40}Ar^*/^{39}Ar$	Age (Ma)	± 1σ.d. (Ma)
650	2.985	1.413	2.85E+03	2.958	28.917	464.231	3.608
700	14.914	5.712	1.15E+04	11.956	30.090	480.755	1.622
720	30.641	7.514	1.52E+04	15.727	30.398	485.075	1.664
730	44.426	6.586	1.33E+04	13.785	30.533	486.952	1.541
740	56.775	5.9	3.08E+02	12.348	30.367	484.635	1.731
750	67.794	5.265	1.06E+01	11.019	30.403	485.141	1.384
760	76.635	4.224	8492	8.842	30.630	488.315	1.452
775	84.109	3.571	2.88E+04	7.474	30.593	487.799	1.857
800	89.947	2.789	6.19E+02	5.837	30.688	489.120	1.663
850	93.253	1.58	1.23E+00	3.307	30.815	490.891	1.767
900	95.354	1.004	3.13E+02	2.101	29.928	478.480	2.927
1000	98.952	1.719	824.8	3.598	30.360	484.540	2.046
1100	99.993	4.975	23.98	1.041	29.863	477.569	5.287
1200	100	3.242	0.06803	0.007	0.001	0.018	861.512

Age determination based on
Lambda K40 = 5.5430E-10
J = 1.0148E-2

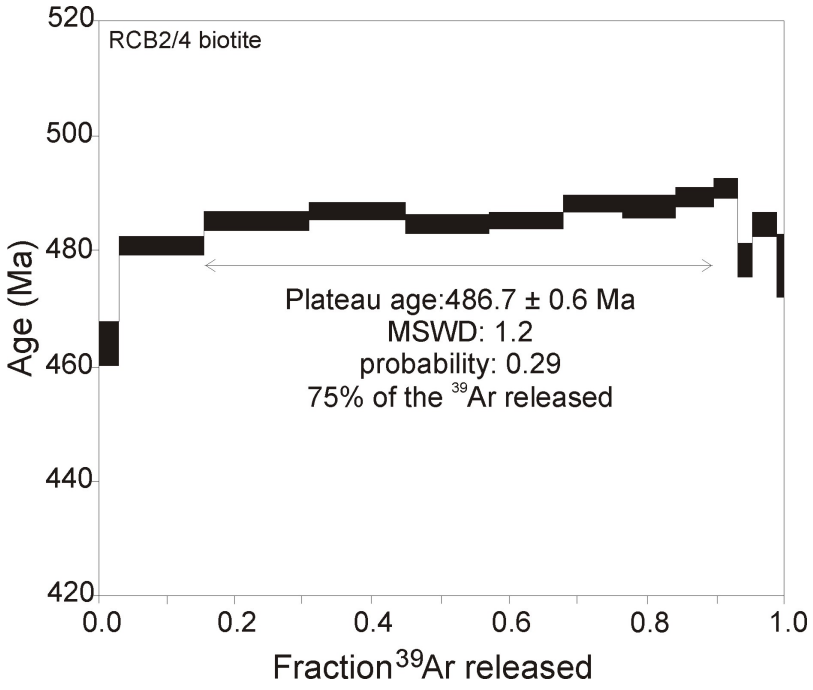

Figure 10. *Age vs. ^{39}Ar released diagram, sample RCB2/4*

Table 8. Data ^{40}Ar-^{39}Ar, sample MJZC9/25 biotite

Temp (C)	Cum $^{\%39}Ar$	$^{40}Ar/^{39}Ar$	$^{37}Ar/^{39}Ar$	$^{36}Ar/^{39}Ar$	Vol. ^{39}Ar $x10^{-15}$mol	%Rad. ^{40}Ar	Ca/K	$^{40}Ar^*/^{39}Ar$	Age (Ma)	± 1σ.d. (Ma)
Mass = 0.30 mg										
J-value = 0.010213 ± 0.000025										
650	1.59	37.07	0.2485	0.0447	0.700	64.3	0.4720	23.84	393.1	6.0
740	19.72	32.73	0.1104	0.0094	7.953	91.4	0.2100	29.92	481.0	1.3
760	37.57	30.95	0.0013	0.0023	7.831	97.6	0.0025	30.21	485.1	2.3
780	54.53	30.63	0.0001	0.0008	7.443	99.0	0.0002	30.34	486.9	1.8
800	67.96	30.65	0.0003	0.0018	5.892	98.1	0.0006	30.06	483.0	1.9
830	77.07	30.91	0.0014	0.0022	3.996	97.7	0.0027	30.20	485.0	1.9
880	82.11	31.83	0.0002	0.0047	2.209	95.4	0.0004	30.37	487.3	4.1
950	90.40	31.62	0.0026	0.0032	3.640	96.8	0.0050	30.61	490.8	1.8
1020	98.10	31.37	0.0013	0.0044	3.376	95.7	0.0024	30.03	482.6	2.0
1100	99.87	35.57	0.0219	0.0198	0.777	83.4	0.0417	29.68	477.6	4.2
1200	99.93	145.75	0.4444	0.5485	0.027	-11.2	0.8450	0.00	0.0	215
1350	100.0	366.26	0.4715	1.2328	0.031	0.5	0.8960	1.77	32.3	804
Total		31.80	0.0257	0.0058	43.87			30.04	482.7	2.8

I) Errors are one sigma uncertainties and exclude uncertainties in the J-value.

ii) Data are corrected for mass spectrometer backgrounds, discrimination and radioactive decay.

iii) Interference corrections: $(^{36}Ar/^{37}Ar)_{Ca}$ = 3.49E-4; $(^{39}Ar/^{37}Ar)_{Ca}$ = 7.86E-4; $(^{40}Ar/^{39}Ar)_K$ = 0.042

iv) J-values are based on an age of 97.9 Ma for GA-1550 biotite.

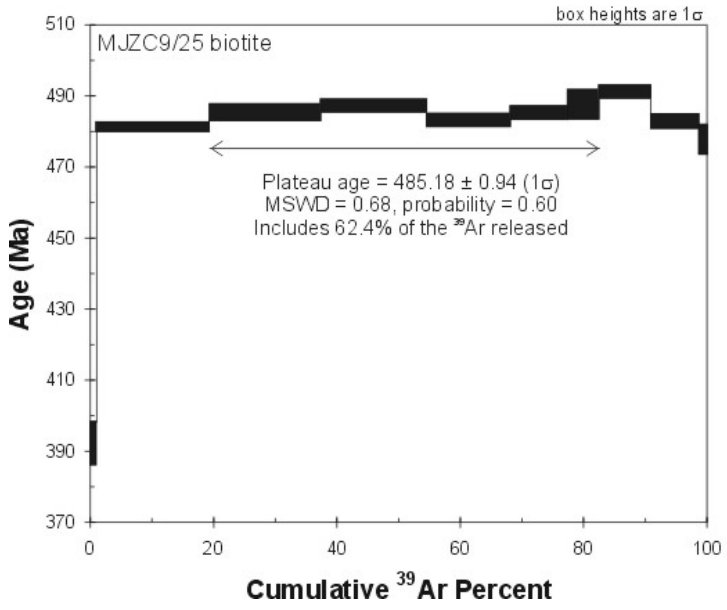

Figure 11. *Age vs. ^{39}Ar released diagram, sample MJZC9/25*

crystals weighing 0.44 mg was analysed. The results are reported in Table 9 and in an age versus $\%^{39}Ar$ released diagram (Fig. 12). The age spectrum presents two young apparent ages (456.4 ± 13.1 and 459.8 ± 6.0 Ma) at the first two temperature steps (600ºC and 680ºC). The following step at 720ºC yields an apparent age at 480.8 ± 3.6 Ma. Apparent ages from step 4 (at 760ºC) to step 12 (at 1300ºC) vary from 491.0 ± 1.6 Ma to 485.4 ± 1.9 Ma. These 9 steps yield, with 97.1% of ^{39}Ar released, a plateau age at 488.0 ± 0.5 Ma with a MSWD at 1.5.

Table 9. Data ^{40}Ar-^{39}Ar, sample NN75/9 biotite

Temp (C)	Cum $\%^{39}Ar$	$^{40}Ar/^{39}Ar$	$^{37}Ar/^{39}Ar$	$^{36}Ar/^{39}Ar$	Vol. ^{39}Ar $x10^{-15}mol$	%Rad. ^{40}Ar	Ca/K	$^{40}Ar^*/^{39}Ar$	Age (Ma)	± 1σ.d. (Ma)
Mass = 0.44 mg										
J-value = 0.010238 ± 0.000036										
600	0.17	51.98	0.2250	0.0806	0.175	54.1	0.4280	28.12	456.4	13.1
680	0.76	38.51	0.1877	0.0343	0.593	73.6	0.3570	28.35	459.8	6.0
720	2.94	32.85	0.0613	0.0100	2.215	90.8	0.1160	29.83	480.8	3.6
760	11.0	31.57	0.0013	0.0043	8.168	95.8	0.0025	30.26	486.8	1.3
780	20.7	31.42	0.0000	0.0027	9.893	97.3	0.0000	30.56	491.0	1.6
800	31.3	31.01	0.0000	0.0021	10.73	97.8	0.0000	30.31	487.5	2.2
830	42.4	30.69	0.0000	0.0014	11.26	98.5	0.0000	30.23	486.4	1.6
860	50.8	30.90	0.0000	0.0023	8.504	97.6	0.0001	30.16	485.4	1.9
900	57.1	31.21	0.0007	0.0029	6.422	97.1	0.0014	30.29	487.3	1.2
960	61.4	31.44	0.0004	0.0039	4.345	96.2	0.0007	30.24	486.5	1.7
1050	76.4	31.06	0.0000	0.0016	15.24	98.2	0.0000	30.51	490.4	1.2
1300	100.0	31.00	0.0000	0.0019	23.94	98.0	0.0000	30.38	488.5	2.0
Total		31.20	0.0030	0.0028	101.50			30.32	487.8	1.8

I) Errors are one sigma uncertainties and exclude uncertainties in the J-value.

ii) Data are corrected for mass spectrometer backgrounds, discrimination and radioactive decay.

iii) Interference corrections: $(^{36}Ar/^{37}Ar)_{Ca}$ = 3.49E-4; $(^{39}Ar/^{37}Ar)_{Ca}$ = 7.86E-4; $(^{40}Ar/^{39}Ar)_{K}$ = 0.042

iv) J-values are based on an age of 97.9 Ma for GA-1550 biotite.

Nchanga, sample NCH1, biotite

Sample NCH1 comes from the lower orebody from Nchanga Mine, in the so-called "Lower Banded Shale" or "LBS" unit, corresponding to the Orebody Formation of the basal Upper Roan Subgroup. It is a graphitic siltstone with quartz, K-feldspar, detrital muscovite and metamorphic biotite. A population of biotite crystals weighing 0.81 mg was analysed with the $^{40}Ar/^{39}Ar$ technique. Results of analyses are reported in an age versus $\%^{39}Ar$ released diagram (Fig. 13) and in Table 10. The first step at 650ºC, yields a younger apparent age at 435.3 ± 2.7 Ma. The steps at 1060ºC and at 1120ºC were lost during manipulation. Steps before and after the loss are similar, within error at 487.7 ± 1.3 Ma and 489.3 ± 3.1 Ma.

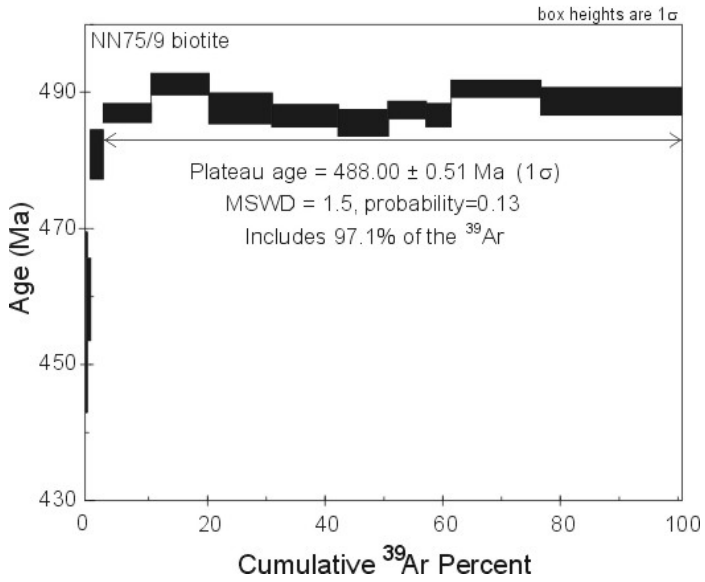

Figure 12. *Age vs. ^{39}Ar released diagram, sample NN75/9*

Table 10. Data ^{40}Ar-^{39}Ar, sample NCH1 biotite

Temp (C)	Cum $^{\%39}Ar$	$^{40}Ar/^{39}Ar$	$^{37}Ar/^{39}Ar$	$^{36}Ar/^{39}Ar$	Vol. ^{39}Ar $x10^{-15}mol$	%Rad. ^{40}Ar	Ca/K	$^{40}Ar^*/^{39}Ar$	Age (Ma)	± 1σ.d. (Ma)
Mass = 0.81 mg										
J-value = 0.010183 ± 0.000025										
650	2.02	28.46	0.0002	0.0055	11.43	94.2	0.0003	26.80	435.3	2.7
720	4.81	32.48	0.0010	0.0035	15.75	96.6	0.0019	31.39	500.4	2.1
780	8.91	31.88	0.0001	0.0017	23.12	98.3	0.0002	31.35	499.8	2.5
820	12.99	31.52	0.0015	0.0017	23.06	98.2	0.0029	30.96	494.4	1.7
850	17.87	30.81	0.0009	0.0011	27.57	98.8	0.0018	30.44	487.1	1.2
880	22.83	30.56	0.0004	0.0010	28.03	98.9	0.0008	30.22	484.0	1.3
910	31.02	30.46	0.0000	0.0007	46.23	99.2	0.0001	30.21	483.9	1.3
940	37.85	30.91	0.0002	0.0010	38.56	98.9	0.0004	30.57	488.9	1.2
980	46.43	30.88	0.0000	0.0012	48.45	98.7	0.0001	30.48	487.7	1.3
1060	67.91	20.71	0.0000	0.0010	121.3	98.4	0.0000	20.38	340.3	1.0
1120	96.88	15.35	0.0000	0.0006	163.7	98.5	0.0000	15.11	258.2	1.5
1180	99.72	34.57	0.0001	0.0133	16.04	88.5	0.0002	30.60	489.3	3.1
1250	100.0	87.24	0.0256	0.1924	1.56	34.8	0.0486	30.36	485.9	20.1
Total		24.47	0.0003	0.0020	564.8			23.84	392.0	1.5

I) Errors are one sigma uncertainties and exclude uncertainties in the J-value.

ii) Data are corrected for mass spectrometer backgrounds, discrimination and radioactive decay.

iii) Interference corrections: $(^{36}Ar/^{37}Ar)_{Ca}$ = 3.49E-4; $(^{39}Ar/^{37}Ar)_{Ca}$ = 7.86E-4; $(^{40}Ar/^{39}Ar)_{K}$ = 0.042

iv) J-values are based on an age of 97.9 Ma for GA-1550 biotite.

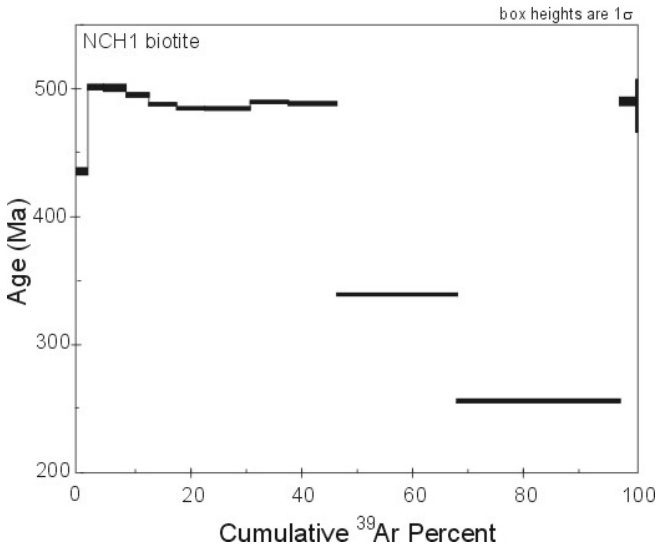

Figure 13. *Age vs. ^{39}Ar released diagram, sample NCH1*

Konkola, sample KN1A, biotite and muscovite

Sample KN1A comes from the Konkola area, northern Zambia. Stratigraphically, it is located in the Lower Roan Subgroup. The sample is a greenish siltstone containing mainly quartz, biotite and muscovite with minor K-feldspar. Analyses of ^{40}Ar-^{39}Ar were done on a population of biotite grains, as well as on a separate population of muscovite grains from the same sample.

- ***Biotite:*** Results of analyses of a biotite population weighing 0.38 mg are reported in Figure 14 and Table 11. The first step at 600°C yielded a young apparent age at 181.6 ± 5.2 Ma (corresponding to 1.57% of ^{39}Ar released). The second apparent age, at 700°C, is older, at 483.7 ± 1.7 Ma (corresponding to 12.68% of the ^{39}Ar released). The five following steps, for temperatures between 740°C and 850°C, give a plateau age at 496.6 ± 0.6 Ma (MSWD = 0.45, 61.5% of ^{39}Ar released) and apparent ages varying between 497.3 ± 1.3 Ma and 494.0 ± 2.1 Ma. The two next steps at temperatures of 920°C and 1100°C yield older apparent ages at 503.2 ± 3.2 Ma and 515.1 ± 2.1 Ma respectively (for a total of 24.0% of ^{39}Ar released). Finally the last step, at 1300°C, yielded a younger apparent age at 342.7 ± 47.7 Ma but corresponds to only 0.22% of the ^{39}Ar released.

- ***Muscovite*****:** A population of muscovite crystals weighing 0.58 mg was analysed. Results are reported in an age spectrum diagram (Fig. 15) and in Table 12. The first step at 700°C, with 5.45% of ^{39}Ar released, yielded an apparent age of 415.1 ± 2.3 Ma. The second step, at 800°C shows a sudden increase of the apparent age at 515.8 ± 1.6 Ma. The third step at 850 °C yielded a younger apparent age than at the previous step, with 489.8 ± 0.7 Ma. From the fourth step (at 900°C) to the eighth step (at 1050°C), the spectrum presents a plateau age at 483.6 ± 1.1 Ma, MSWD = 2.1, corresponding to 69.4% of the ^{39}Ar released with apparent ages varying from 485.4 ± 1.3 Ma to 481.5 ± 1.0 Ma.

Table 11. Data ^{40}Ar-^{39}Ar, sample KN1A biotite

Temp (C)	Cum $^{\%39}Ar$	$^{40}Ar/^{39}Ar$	$^{37}Ar/^{39}Ar$	$^{36}Ar/^{39}Ar$	Vol. ^{39}Ar $x10^{-15}$mol	%Rad. ^{40}Ar	Ca/K	$^{40}Ar^*/^{39}Ar$	Age (Ma)	± 1σ.d. (Ma)
Mass = 0.38mg										
J-value = 0.010256 ± 0.000025										
600	1.57	19.85	0.0513	0.0320	1.197	52.0	0.0975	10.33	181.6	5.2
700	14.25	33.18	0.0763	0.0107	9.701	90.3	0.1450	29.98	483.7	1.7
740	31.52	31.43	0.0027	0.0016	13.21	98.3	0.0052	30.90	496.6	1.4
760	46.29	31.31	0.0000	0.0012	11.29	98.6	0.0000	30.88	496.3	1.4
780	58.84	31.40	0.0000	0.0014	9.595	98.4	0.0001	30.92	496.9	1.3
810	70.22	31.37	0.0007	0.0012	8.709	98.7	0.0013	30.95	497.3	1.3
850	75.76	31.60	0.0023	0.0028	4.231	97.2	0.0044	30.72	494.0	2.1
920	82.26	32.46	0.0042	0.0035	4.972	96.7	0.0080	31.37	503.2	3.2
1100	99.78	33.05	0.0033	0.0026	13.40	97.5	0.0064	32.22	515.1	2.1
1300	100.0	85.75	0.1986	0.2210	0.168	23.8	0.3770	20.40	342.7	47.7
Total		31.92	0.0125	0.0040	76.48			30.69	493.7	1.9

I) Errors are one sigma uncertainties and exclude uncertainties in the J-value.

ii) Data are corrected for mass spectrometer backgrounds, discrimination and radioactive decay.

iii) Interference corrections: $(^{36}Ar/^{37}Ar)_{Ca}$ = 3.49E-4; $(^{39}Ar/^{37}Ar)_{Ca}$ = 7.86E-4; $(^{40}Ar/^{39}Ar)_{K}$ = 0.042

iv) J-values are based on an age of 97.9 Ma for GA-1550 biotite.

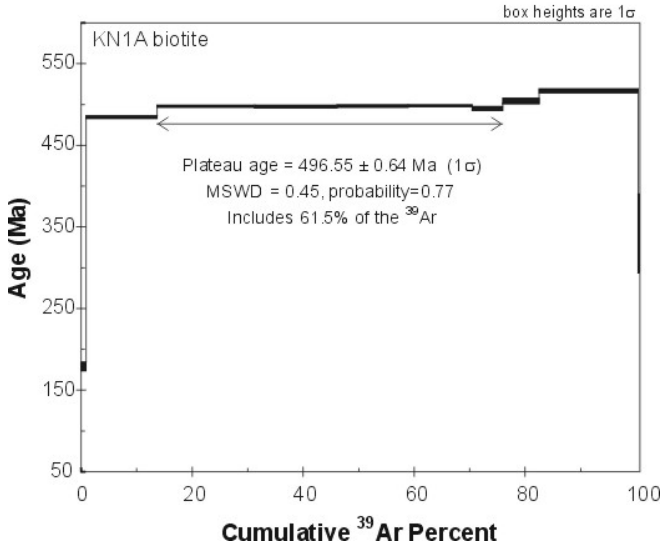

Figure 14. *Age vs. ^{39}Ar released diagram, sample KN1A biotite*

Table 12. Data ^{40}Ar-^{39}Ar, sample KN1A muscovite

Temp (C)	Cum $^{\%39}Ar$	$^{40}Ar/^{39}Ar$	$^{37}Ar/^{39}Ar$	$^{36}Ar/^{39}Ar$	Vol. ^{39}Ar $x10^{-15}$mol	%Rad. ^{40}Ar	Ca/K	$^{40}Ar^*/^{39}Ar$	Age (Ma)	± 1σ.d. (Ma)
Mass = 0.58 mg										
J-value = 0.010252 ± 0.000036										
700	5.45	27.32	1.5448	0.0075	2.983	92.3	2.940	25.24	415.1	2.3
800	16.33	32.78	0.3712	0.0017	5.948	98.4	0.706	32.28	515.8	1.6
850	29.36	31.07	0.0198	0.0020	7.117	97.9	0.038	30.42	489.8	0.7
900	49.87	30.57	0.0171	0.0015	11.21	98.3	0.033	30.08	484.9	1.1
930	66.73	30.29	0.0326	0.0014	9.215	98.5	0.062	29.84	481.5	1.0
960	80.03	30.73	0.0450	0.0024	7.264	97.5	0.086	29.94	483.0	1.2
1000	91.28	31.05	0.2201	0.0031	6.151	97.0	0.418	30.12	485.4	1.3
1050	98.73	31.43	0.1670	0.0046	4.072	95.5	0.317	30.02	484.1	1.9
1140	99.72	40.76	2.4402	0.0401	0.539	71.4	4.650	29.15	471.7	4.4
1380	100.0	121.39	5.1430	0.3090	0.154	25.2	9.810	30.68	493.3	45.3
Total		31.14364	0.2181	0.0037	54.65			30.03	484.3	1.4

I) Errors are one sigma uncertainties and exclude uncertainties in the J-value.

ii) Data are corrected for mass spectrometer backgrounds, discrimination and radioactive decay.

iii) Interference corrections: $(^{36}Ar/^{37}Ar)_{Ca}$ = 3.49E-4; $(^{39}Ar/^{37}Ar)_{Ca}$ = 7.86E-4; $(^{40}Ar/^{39}Ar)_K$ = 0.042

iv) J-values are based on an age of 97.9 Ma for GA-1550 biotite.

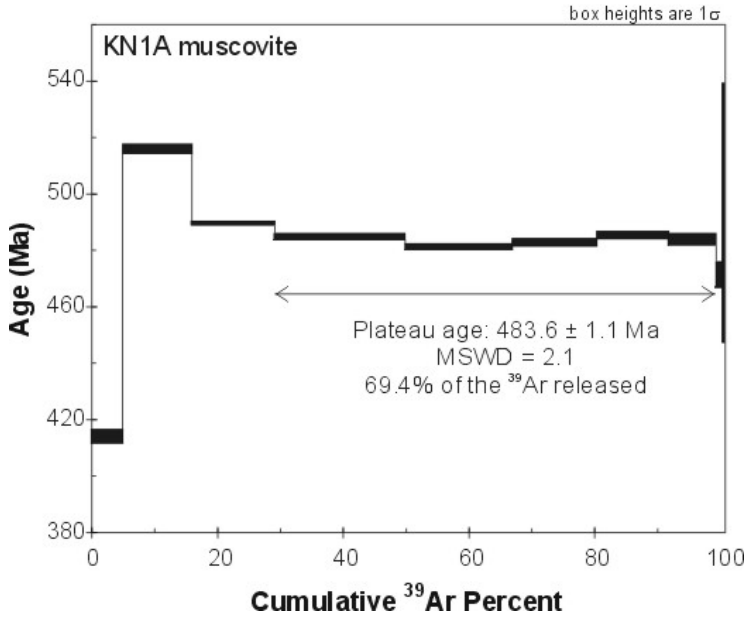

Figure 15. *Age vs. ^{39}Ar released diagram, sample KN1A muscovite*

Musoshi (DRC), sample MUS 1, microcline

Sample MUS1 comes from the Musoshi Mine in the Democratic Republic of Congo. It is an arkose which was located in the Musoshi Formation of the Lower Roan Subgroup, which forms a part of the footwall of the orebody in the Musoshi area. A population of microcline grains, weighing 0.81 mg, was separated and analysed with the ^{40}Ar-^{39}Ar technique. Results are reported in Table 13 and in an age spectrum, age versus ^{39}Ar released diagram (Fig. 16). Apparent ages vary between 405.8 ± 3.8 Ma and 467.0 ± 2.7 Ma.

Table 13. Data ^{40}Ar-^{39}Ar, sample MUS1 microcline

Temp (C)	Cum $^{\%39}Ar$	$^{40}Ar/^{39}Ar$	$^{37}Ar/^{39}Ar$	$^{36}Ar/^{39}Ar$	Vol. ^{39}Ar $x10^{-15}$mol	%Rad. ^{40}Ar	Ca/K	$^{40}Ar^*/^{39}Ar$	Age (Ma)	± 1σ.d. (Ma)
Mass = 0.30 mg										
J-value = 0.010188 ± 0.000025										
650	1.66	30.33	0.0063	0.0187	1.287	81.6	0.0119	24.76	405.8	3.8
750	6.68	27.93	0.0001	0.0055	3.878	93.9	0.0001	26.23	427.3	2.8
840	12.79	28.28	0.0000	0.0035	4.728	96.2	0.0001	27.19	441.1	2.2
900	17.46	28.92	0.0009	0.0036	3.606	96.1	0.0016	27.79	449.8	2.4
950	21.65	28.64	0.0010	0.0043	3.243	95.4	0.0019	27.32	442.9	1.5
1000	26.78	28.73	0.0001	0.0040	3.964	95.7	0.0001	27.50	445.6	1.8
1050	33.42	28.34	0.0004	0.0034	5.137	96.3	0.0007	27.29	442.6	2.2
1100	41.94	28.55	0.0000	0.0031	6.589	96.6	0.0001	27.58	446.8	1.8
1150	56.54	28.48	0.0002	0.0024	11.29	97.3	0.0003	27.72	448.8	2.4
1175	69.76	28.54	0.0000	0.0024	10.22	97.3	0.0001	27.75	449.2	1.3
1200	83.91	28.67	0.0000	0.0014	10.95	98.3	0.0000	28.21	455.7	1.3
1225	93.35	29.32	0.0004	0.0027	7.303	97.1	0.0007	28.47	459.4	1.9
1260	97.14	30.45	0.0001	0.0059	2.927	94.1	0.0002	28.66	462.2	2.3
1300	98.90	33.81	0.0014	0.0161	1.358	85.8	0.0026	29.00	467.0	2.7
1350	99.60	45.54	0.0045	0.0590	0.547	61.6	0.0086	28.05	453.5	7.4
1400	100.0	60.90	0.0127	0.1179	0.306	42.7	0.0242	26.03	424.3	8.6
Total		29.05	0.0004	0.0043	77.32			27.70	448.4	2.0

I) Errors are one sigma uncertainties and exclude uncertainties in the J-value.

ii) Data are corrected for mass spectrometer backgrounds, discrimination and radioactive decay.

iii) Interference corrections: $(^{36}Ar/^{37}Ar)_{Ca}$ = 3.49E-4; $(^{39}Ar/^{37}Ar)_{Ca}$ = 7.86E-4; $(^{40}Ar/^{39}Ar)_{K}$ = 0.042

iv) J-values are based on an age of 97.9 Ma for GA-1550 biotite.

DISCUSSION

The deposition of the Katangan sequence started somewhere after 877 Ma (Armstrong *et al*., 2004) and finished sometime after 573 ± 5 Ma (Master *et al*., 2005). Following deposition, the Katangan sedimentary sequence underwent several episodes of metamorphism during the late Neoproterozoic Pan-African Lufilian Orogeny, which gave the Copperbelt its arcuate shape (Cahen *et al*., 1984; Cosi *et al*., 1992).

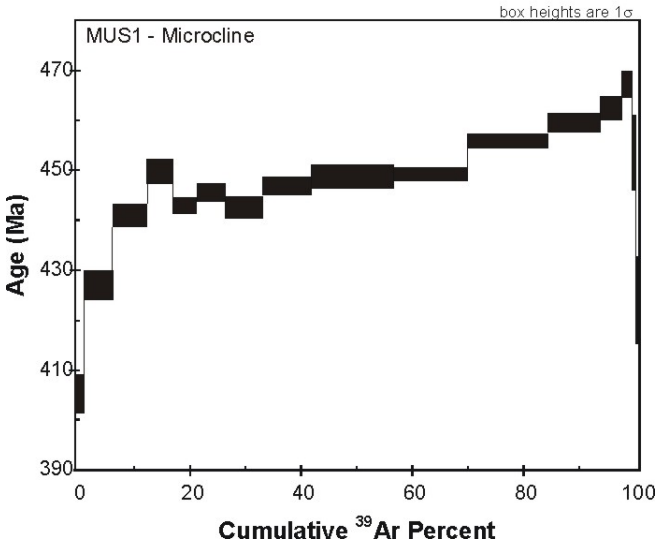

Figure 16. *Age vs. ^{39}Ar released diagram, sample MUS1.*

Geochronology

^{40}Ar-^{39}Ar analyses of all biotite, muscovite and microcline samples yielded degassing patterns with well-known features. All the samples showed very young apparent ages associated with low temperatures of degassing. These young apparent ages can be related to the release of the argon located in the external, least retentive sites of the minerals. The energy necessary to release the argon in these sites is minimal and the slightest thermal disturbance could produce a loss of argon (Hanes, 1991). A common feature in biotite degassing patterns is the presence of two peaks in the apparent ages at 680°C and 850°*C.* The first peak at around 650°C represents released argon related to a stage of dehydroxylation of the biotite, while the second peak at 850°C can be related to one phase of dehydroxylation of chlorite (Lo and Onstott, 1989).

The justification for using two methods of analyses lies in the difference between their closure temperatures. For the biotite and muscovite and in the case of ^{40}Ar-^{39}Ar analyses, closure temperatures are between 300-400°*C.* For monazite in U-Pb analyses, Parrish (1990) evaluated the closure temperature at 725 ± 25 °C, while more recent studies (Cherniak *et al*., 2002) estimate it at more than 900 °*C.* Hence, ages obtained for analyses on monazite give the age of crystallisation of these minerals or the age of a metamorphic event in the case of overgrowths. As seen in the samples analysed, monazites commonly do not lie on the Concordia curve. This behaviour is attributed to the presence of excess ^{206}Pb formed by the initial incorporation of ^{230}Th (Heaman and Parrish, 1991). Ages obtained using the ^{40}Ar-^{39}Ar technique are not as straightforward to interpret. While a plateau age gives the age of a metamorphic event, in general, ages produced with the ^{40}Ar-^{39}Ar technique commonly generate problems of interpretation.

In this study, ten populations of biotite, muscovite and microcline grains were analysed using the ^{40}Ar-^{39}Ar technique. Out of these ten samples, three (NN75/26, NCH1 and MUS1) do not yield plateau ages as defined by MacDougall (1999). In this section we discuss the provisos related to the interpretation of these three samples. Sample NN75/26, which was collected from an iron-formation located 2 m below a tuffaceous layer, yielded a hump-shaped curve on an age vs %^{39}Ar released diagram, with apparent ages ranging from 53.7 ± 1.0 Ma to 631.8 ± 1.8 Ma, which implies a thermal disturbance of

the system (Lo and Onstott, 1989; Di Vicenzo *et al*., 2003). The maximum apparent ages of this sample are significantly older than ages yielded by other samples from this area and from this drill hole. The 631.8 ± 1.8 Ma apparent age is the highest recorded during this study but is difficult to interpret because it occurs without the presence of a plateau age. Still, this age can be found elsewhere in the Lufilian Arc (Cosi *et al*., 1992). One plausible explanation for the disturbed age spectrum yielded by the sample NN75/26 is the incorporation of an excess of argon in the biotite. It is difficult to pin-point the cause of this excess. The emplacement of the tuffaceous layer below which the sample was extracted cannot explain this argon excess. The temperatures involved were too low and the thermal effects on the surrounding rocks were minimal. Although the biotite was separated with extreme care in order to obtain pristine biotite, it is possible that some chloritised biotite may have been included in the analysed population of grains. The excess of argon may then have been associated with the chlorite (Lo and Onstott, 1989). Problems with the sample NCH1 from Nchanga Mine were purely technical and induced a partial loss of argon. It should be noted that the apparent age before the loss, 487.7 ± 1.3 Ma, is similar within error, to the apparent age following the lost step due to the technical problem, at 489.3 ± 3.1 Ma. Finally, microclines (from sample MUS1) were also analysed with the ^{40}Ar-^{39}Ar technique. This sample does not yield a plateau age but instead shows gradually increasing apparent ages between 405.8 ± 3.8 Ma and 467.0 ± 2.7 Ma. It is not uncommon to find these age spectra for potassium feldspars. These minerals do not have one closure temperature but a range of closure temperatures ranging from 350°C to 125°C (Foland, 1974; Purdy and Jäger, 1976; Harrison and McDougall, 1982; Lovera *et al*., 1989). A spectrum without a plateau age may imply a slow cooling, but it is difficult to quantify the rate at which it occurs without a complete ^{40}Ar-^{39}Ar study of K-feldspars from the area.

Table 14. Summary of the ages obtained

U-Pb technique

Sample name	**Mineral**	**Plateau age**	**Age (Ma)**
RCB2/72	monazite	N/A	592 ± 22
RCB1/36	monazite	N/A	531 ± 12
RCB2/112	monazite	N/A	512 ± 17

^{40}Ar-^{39}Ar technique

Sample name			
BH89/3	biotite	yes	586.1 ± 1.7
NN75/26	biotite	no	between 53.7 ± 1.0 and 631.8 ± 1.8
RCB2/112	biotite	yes	491.5 ± 1.6
RCB2/4	biotite	yes	490.9 ± 0.6
MJZC9/25	biotite	yes	485.2 ± 0.9
NN75/9	biotite	yes	488.0 ± 0.5
NCH1	biotite	no	between 435.3 ± 2.7 and 499.8 ± 2.5
KN1A	biotite	yes	496.6 ± 0.6
KN1A	muscovite	yes	483.6 ± 1.1
MUS1	microcline	no	between 405.8 ± 3.8 and 467.0 ± 2.7

In the present study, Ar-Ar and U-Pb SHRIMP analyses were performed on several samples collected from a stratigraphic succession extending from the Lower Roan Subgroup to the Grand Conglomerat Formation. A summary of the ages obtained in this study is given in Table 14. The ages obtained do not represent a continuum but rather several distinct groupings. Three samples yielded ages between 631.8 ± 1.8 and 592 ± 22 Ma. This age span is recorded in other parts of the Central African Copperbelt and in the Irumide Belt. In central Zambia a phase of eclogite facies metamorphism was dated at 595 ± 10 Ma, based on a Sm-Nd age on garnet and whole rock in eclogite (John *et al*., 2003). In the Zambian Copperbelt, Re-Os analyses on rocks from the Nkana, Chibuluma and Nchanga deposits yielded an isochron age of 583 ± 24 Ma (Barra *et al*., 2004). A similar, but reset, Rb-Sr age of 582 ± 40 Ma was obtained (Cahen *et al*., 1984) for the Kafue Rhyolite, which has a U-Pb zircon age of *c.* 879 Ma (Hanson *et al*., 1994). U-Th-Pb analyses on monazites from the Luiswishi Cu-Co-U deposits in the Democratic Republic of Congo gave ages between 603 ± 31 Ma and 556 ± 29 Ma (Lerouge *et al*., 2004). The age of 531 ± 12 Ma obtained in this study with the U-Pb technique on metamorphic monazites from the Chambishi basin is similar to others found elsewhere in the Lufilian arc and the Zambezi Belt. Monazite from a biotite-kyanite-garnet gneiss showed an U-Pb age of 529 ± 2 Ma while the same minerals from some whiteschists yielded $^{207}Pb/^{235}U$ ages of 531 to 532 ± 2 Ma (John *et al*., 2004). Molybdenite from the Nkana deposit yielded an age of 525.7 ± 3.4 Ma with the Re-Os technique (Barra *et al*., 2004). In central Zambia, an unfolded rhyolite in the Katangan sedimentary sequence was dated with the U-Pb zircon leaching technique at 538.0 ± 1.5 Ma (Hanson *et al*., 1993). Recent U-Th-Pb analyses on monazites of sediments from the Luiswishi deposit yielded an age of 556 ± 29 Ma (Lerouge *et al*., 2004). Analyses on monazites and rutiles from the Kalumbila deposit in northwest Zambia yielded U-Pb ages of 548.6 ± 7.6 Ma and 531 ± 21 Ma respectively (Steven and Armstrong, 2003). The age of 512 ± 17 Ma, obtained from the last set of analysed monazites (RCB1/36), was also found elsewhere in the Copperbelt. Richards *et al*. (1988a, b) analysed rutiles and uraninites associated with veining crosscutting the ore body of the Musoshi deposit. The ages for rutile and uraninite are identical with 514 ± 2 Ma and 514 ± 3 Ma. More recently, Re-Os and U-Pb analyses of respectively molybdenite and monazite yielded ages of 511.8 ± 1.7 Ma (molybdenite), 512.9 ± 1.7 Ma (molybdenite) and 509 ± 11 Ma (monazite) (Torrealday *et al*., 2000).

The last and largest set of samples yielded the youngest age range, between 467.0 ± 2.7 Ma and 496.6 ± 0.6 Ma. Similar ages are widely recorded in the Copperbelt and adjacent areas. In the Domes area, west of the Zambian Copperbelt, Cosi *et al*. (1992) obtained a large set of K-Ar and Rb-Sr ages ranging from 475 ± 6 Ma to 492 ± 6 Ma. Furthermore, Cahen and Snelling (1971) obtained a K-Ar age of 483 ± 15 Ma for lavas located in the Kibambale area as well as K-Ar biotite ages from Nkana, Nchanga and Kinsenda ranging between 495 and 422 Ma.

Regional implications

During the Neoproterozoic, at *c.* 750–730 Ma, the southern part of the Congo Craton underwent rifting during the opening of the Khomas ocean (Hoffman, 1994). Damaran and Katangan sedimentary rocks were deposited in the resulting passive margin (Porada and Berhorst, 2000). During the Pan-African Damaran-Lufilian Orogeny, the Khomas ocean closed with subduction of oceanic lithosphere underneath the Congo Craton margin, leading to the formation of an Andean-type magmatic arc, and ultimately to the Himalayan-type collision between the Congo and Kalahari Cratons at about 550-510 Ma (Miller, 1983; Porada and Berhorst, 2000). Eclogite facies metamorphism from the Zambezi Belt, dated at 595 ± 10 Ma, and comprising associated gabbros, metagabbros and eclogite, records the timing of the subduction, which took place in an oceanic environment (John *et al*., 2003).

The ages of *c.* 590 Ma recorded by both the U-Pb system in monazite, and the ^{40}Ar-^{39}Ar system in biotite in the present study show that there was some tectonic activity with attendant metamorphism in the Chambishi Basin that was coeval with the eclogite facies metamorphism recorded in the Zambezi Belt. The temperatures during this first metamorphic event were higher than during subsequent events, as recorded by the epidote-amphibolite facies assemblages at Muliashi. Talc-kyanite whiteschists in the Lufilian Arc, dated at *c.* 530 Ma, represent the final stage of collision between the Congo and the Kalahari Cratons (John *et al*., 2004). Our monazite age of 531 ± 12 Ma is probably related to this event. The ages at *c.* 512 Ma recorded in the Katangan basin are clearly related to a widespread mineralising phase (molybdenite, monazite, rutile, uraninite) due to circulation of fluids (Richards *et al*., 1988a,b; Torrealday *et al*., 2000). The range of ^{40}Ar-^{39}Ar mica ages at *c.* 492–406 Ma may be related to post-orogenic regional uplift and cooling which affected the whole Katangan basin. The youngest apparent $^{40}Ar/^{39}Ar$ ages obtained are from microcline at Musoshi and range from 467.0 ± 2.7 Ma to 405.8 ± 3.8 Ma. This age range encompasses a muscovite Rb-Sr age of 450 ± 9 Ma from Malundwe in the Mwombezhi Dome (Cosi *et al*., 1992). This young metamorphic event corresponds to the age (458–427 Ma) of the late nepheline-syenite Mukumbi intrusion north of the Mwombezhi Dome (Cosi *et al*., 1992). Young intrusions of an age similar to the Mukumbi nepheline-syenite have not been reported from the Copperbelt region, thus it is likely that the youngest ages recorded by the microclines at Musoshi are a reflection of continued post-orogenic uplift and slow cooling of the Lufilian orogen.

ACKNOWLEDGEMENTS

The authors thank Claus Schlegel (Avmin Zambia), Tumba Tshiauka (Musoshi Mine, DRC), and the staff of Mufulira, Nchanga and Muliashi South mines and the Kalulushi core yard for access to the samples. We are grateful to Dr. Steve Prevec for his insightful and timeous review of this paper.

REFERENCES

Armstrong, R.A., Robb, L.J., Master, S., Kruger, F.J., Mumba, P.A.*C.C.*, 1999. New U-Pb age constraints on the Katangan Sequence, Central African Copperbelt. Journal of African Earth Sciences 28(4A), 6-7.

Armstrong, R.A., 2000. Ion microprobe (SHRIMP) dating of zircons from granites, granulites and volcanic samples from Zambia. Unpubl. Rep., ANU, PRISE Job No. A99-160, Canberra.

Barra, F., Broughton, D., Ruiz, J., Hitzman, M., 2004. Multi-stage mineralization in the Zambian Copperbelt based on Re-Os isotope constraints. Denver Annual Meeting, November 7-10, Geological Society of America Abstract with Programs, 36 (5).

Cahen, L., Francois, A., Ledent, D., 1971. Sur l'âge des uraninites de Kambove ouest et de Kamoto Principal et révisions des connaissances aux minéralisations uranifères du Katanga et du Copperbelt de Zambia. Annales de la Société Géologique de Belgique 94, 185-198.

Cahen, L., Snelling, N.J., 1971. Données radiométriques nouvelles par la méthode potassium-argon. Existence d'une importante élévation post-tectonique de la température dans les couches katangiennes du Sud du Katanga et du Copperbelt de la Zambie. Annales de la Société Géologique de Belgique 94, 199-209.

Cailteux, J.L.H., 2003. Comment from the Organizer. In: Guide-Book to the Field Trip, IGCP No. 450, Proterozoic Sediment-hosted Base Metal Deposits of Western Gondwana; Conference and Field Workshop Lubumbashi 2003, Lubumbashi, D.R. Congo, 204-205.

Cailteux, J.L.H., Kampunzu, A.B., Ngoie Bwanga, F., 2003. Lithostratigraphy of the Mwashya Subgroup in Congo (Central African Copperbelt), with special reference to the Luiswishi area. In: Contributions presented at the 3rd IGCP-450 Conference, Proterozoic Sediment-hosted Base Metal Deposits of Western Gondwana; Conference and Field Workshop Lubumbashi 2003, Lubumbashi, D.R. Congo, 83-87.

Cherniak, D. J., Watson, E. B., Grove, M., Harrison, T. M., 2002. Pb diffusion in monazite. Abstract volume, The Geological Society of America Annual Meeting, Denver 2002, October 27-30, Paper 138-5.

Claoué-Long, J.*C.*, Compston, W., Roberts, J., Fanning, *C.*M., 1995. Two carboniferous ages: a comparison of SHRIMP zircon dating with conventional zircon ages and $^{40}Ar/^{39}Ar$ analysis. In: Geochronology Time Scales and Global Stratigraphic Correlation, SEPM Special Publication No 54, 1-21.

Cosi, M., DeBonis, A., Gosso, G., Hunziker, J., Martinotti, G., Moratto, S., Robert, J.P., Ruhlman, F., 1992. Late Proterozoic thrust tectonics, high-pressure metamorphism and uranium mineralization in the Domes area, Lufilian arc, northwestern Zambia. Precambrian Research 58, 215-240.

Di Vincenzo, G., Viti, *C.*, Rocchi, S., 2003. The effect of chlorite interlayering on ^{40}Ar-^{39}Ar biotite dating: an ^{40}Ar-^{39}Ar laser-probe and TEM investigations of variably chloritised biotites. Contributions to Mineralogy and Petrology 145, 643-658.

Foland, K.A., 1974. ^{40}Ar diffusion in homogenous orthoclase and an interpretation of Ar diffusion in K-feldspar. Geochimica et Cosmochimica Acta 38, 151-166.

François, A., 1974. Les minéralisations du Shaba méridional et leur environement lithologique et tectonique. In: Bartholomé, P., de Magnée, I., Evrard, P., Moreau, J. (Ed.), Gisements stratiformes et Provinces cuprifères*,* Société géologique de Belgique, Liège, 79-101.

Hanes, J. A., 1991. K-Ar and ^{40}Ar-^{39}Ar geochronology: methods and applications. In*:* Heaman, L., Ludden, J.N., (Eds.), Short course handbook on applications of radiogenic isotope systems to problems in geology. Mineralogical Association of Canada 19, 27-57.

Hanson, R.E., Wardlaw, M.S., Wilson, T.J., Mwale, G., 1993. U-Pb zircon ages from the Hook granite massif and Mwembeshi dislocation: constraints on Pan-African deformation, plutonism, and transcurrent shearing in central Zambia. Precambrian Research 63, 189-209.

Hanson, R.E., Wilson, T.J., Munyanyiwa, H., 1994. Geologic evolution of the Neoproterozoic Zambezi Orogenic Belt in Zambia. Journal of African Earth Sciences 18, 135-150.

Harrison, T.M., McDougall, I., 1982. The thermal significance of potassium feldspar K-Ar ages spectrum results. Geochimica et Cosmochimica Acta 46, 1811-1820.

Heaman, L., Parrish, R., 1991. U-Pb geochronology of accessory minerals. In*:* Heaman, L., Ludden, J.N., (Eds.), Short course handbook on applications of radiogenic isotope systems to problems in geology. Mineralogical Association of Canada 19, 59-102.

Hoffman, K.-H., 1994. New constraints on the timing of continental breakup and collision in the Damara Belt. Conference on Proterozoic Crustal and Metallogenic Evolution, 29 August- 1 September, 1994, Windhoek, Namibia, p. 30.

JICA/MMAJ, 1996. Report on the cooperative mineral exploration in the Chambishi Southeast Area, the Republic of Zambia. Consolidated Report, February 1996, 157 pp + Appendices.

John, T., Schenk, V., Haase, K., Scherer, R., Tembo, F., 2003. Evidence for a Neoproterozoic ocean in south-central Africa from mid-oceanic-ridge-type geochemical signatures and pressure-temperature estimates of Zambian eclogites. Geology 31, 3, 243-246.

John, T., Schenk, V., Mezger, K., Tembo, F., 2004. Timing and PT evolution of whiteschist metamorphism in the Lufilian arc-Zambezi belt orogen (Zambia): implications for the assembly of Gondwana. The Journal of Geology 112, 71-90Kampunzu, A.B., Wendorff, M., Kruger, F.J., Intiomale, M.M., 1998. Pb isotopic ages of sediment-hosted Pb-Zn mineralisation in the Neoproterozoic Copperbelt of Zambia and Democratic Republic of Congo (ex-Zaire): re-evaluation and implications. Chronique de Recherche Minière 530, 55-61

Key, R.M., Liyungu, A.K., Njamu, F.M., Somwe, V., Banda, J., Mosley, P.N., Armstrong, R.A., 2001. The Western arm of the Lufilian Arc, NW Zambia and its potential for copper mineralization. Journal of African Earth Sciences 33 (3-4), 503-528.

Lerouge, *C.*, Cocherie, A., Cailteux, J., Kampunzu, A.B., Breton, J., Gilles, *C.*, Milési, J.-P., 2004. Preliminary U-Th-U electron microprobe dating of monazite: chronological constraints on the genesis of the Luiswishi Cu-Co-U ore deposit, D. R. Congo. Geosciences Africa 2004, Abstract Volume 1, University of the Witwatersrand, Johannesburg, South Africa, 382-383.

Liyungu, A.K., Mosley, P.N., Njamu, F.M., Banda, J., 2001. Geology of the Mwinilunga area. Report of the Geological Survey of Zambia 110, 36 pp.

Lo, *C.*-H., Onstott, T.*C.*, 1989. ^{39}Ar recoil artefact in chloritized biotite. Geochimica et Cosmochimica Acta 53, 2697-2711.

Lovera, O.M., Richter, F.M., Harrison, T.M., 1989. The $^{40}Ar/^{39}Ar$ thermochronometry for slowly cooled samples having a distribution of diffusion domain sizes. Journal of Geophysical Research 94B, 17917-17935.

Ludwig, K.R., 2000. Users Manual for Isoplot/Ex version 2.3, a geochronological toolkit for Microsoft Excel. Berkeley Geochronology Center, Special Publications 1a.

MacDougall, I., Harrison, T.M., 1999. Geochronology and thermochronology by the $^{40}Ar/^{39}Ar$ method. Second Edition. Oxford University Press, New York.

Master, S., Rainaud, *C.*, Armstrong, R. A., Phillips, D., Robb, L. J., 2005. Provenance ages of the Neoproterozoic Katanga Supergroup (Central African Copperbelt), with implications for basin evolution. Journal of African Earth Sciences, (this issue).

Mbendi, Information for Africa., 2002. Zambia – Mining: Copper Mining – Overview. Internet Web site: www.mbendi.co.za/indy/ming/cppr/af/za/p0005.html.

Mendelsohn, F., 1961. Metamorphism. In: Mendelsohn, F. (Ed.), The Geology of the Northern Rhodesian Copperbelt. Macdonald, London, 106-116.

Porada, H., Berhorst, V., 2000. Towards a new understanding of the Neoproterozoic-Early Palaeoproterozoic Lufilian and northern Zambezi Belts in Zambia and the Democratic Republic of Congo. Journal of African Earth Sciences 30, 727-771.

Purdy, J.W., Jäger, E., 1976. K-Ar ages on rock-forming minerals from the Central Alps. Report of the Institute of Geology and Mineralogy, University of Padova 30, 1-31

Rainaud, *C.*, Master, S., Armstrong, R.A., Robb, L.J., 2003. A cryptic mesoarchaean terrane in the basement to the central African Copperbelt. Journal of the Geological Society, London 160, 11-14.

Rainaud, *C.* Master, S., Armstrong, R.A., Robb, L.J., 2005. Geochronology and nature of the Palaeoproterozoic Basement in the Central African Copperbelt (Zambia and Democratic Republic of Congo), with regional implications. Journal of African Earth Sciences, (this issue).

Richards, J.P., Cummings, G.L., Krstic, D., Wagner, P.A., Spooner, E.T.*C.*, 1988a. Pb isotope constraints on the age of sulfide ore deposition and U-Pb age of late uraninite veining at the Musoshi stratiform copper deposit, Central African Copperbelt, Zaire. Economic Geology 83, 724-741.

Richards, J.P., Krogh, T.E., Spooner, E.T.*C.*, 1988b. Fluid inclusion characteristics and U-Pb rutile age of late hydrothermal alteration and veining at the Musoshi stratiform copper deposit, Central African Copperbelt, Zaire. Economic Geology 83, 118-139.

Spell, T.L., McDougall, I., 2003. Characterization and calibration of $^{40}Ar/^{39}Ar$ dating standards. Chemical Geology 198, 189-211.

Steiger, R.H., Jäger, E., 1977. Subcommission on geochronology: convention on the use of decay constants in geo- and cosmochronology. Earth and Planetary Science Letters 36, 359-362.

Steven, N., Armstrong, R.A., 2003. A metamorphosed Proterozoic carbonaceous shale-hosted Co-Ni-Cu deposit at Kalumbila, Kabompo Dome: the Copperbelt ore shale in northwest Zambia. Economic Geology 98, 893-909.

Tetley, N., MacDougall, I., Heydegger, H.R., 1980. Thermal neutron interferences in the $^{40}Ar/^{39}Ar$ dating technique. Journal of Geophysical Research 85, 7201-7205.

Torrealday, H.I., Hitzman, M.W., Stein, H.J., Markey, R.J., Armstrong, R., Broughton, D., 2000. Re-Os and U-Pb dating of the vein-hosted mineralization at the Kansanshi copper deposit, northern Zambia. Economic Geology 95, 1165-1170

Walraven, F., Chabu, M., 1994. Pb-isotope constraints on base-metal mineralisation at Kipushi (Southeastern Zaïre). Journal of African Earth Sciences 18, 1, 73-82.

Wendorff, M., 2001a. New exploration criteria for 'megabreccia'-hosted Cu-Co deposits in the Katangan Belt, central Africa. In: Piestrzynski, A. *et al*. (Eds.), Mineral Deposits at the Beginning of the 21st Century. Swets & Zeitlinger Publishers, Lisse, Netherlands, 19-22.

Wendorff, M., 2001b. Evolution of the Katangan Belt foreland basins: Neoproterozoic-Lower Palaeozoic of Zambia and the Democratic Republic of Congo. Abstract, 21st IAS-Meeting of Sedimentology, 3 - 5 September 2001, Davos, Switzerland.

Wendorff, M., 2002a. Megabreccias of the Katangan orogen (Neoproterozoic-Lower Palaeozoic of Central Africa): criteria for re-interpretation as synorogenic conglomerates. 16th International Sedimentological Congress, Abstracts Volume, Rand Afrikaans University, Johannesburg, South Africa, 395-396.

Wendorff, W., 2002b. Synorogenic conglomerates and evolution of foreland basins in the external fold-thrust belt of the Katangan orogen, Neoproterozoic-L. Palaeozoic of Zambia and the Democratic Republic of Congo. 16th International Sedimentological Congress, Abstracts Volume, Rand Afrikaans University, Johannesburg, South Africa, 397-398.

Wendorff, M., 2003a. Stratigraphy of the Fungurume Group- evolving foreland basin succession in the Lufilian fold-thrust belt, Neoproterozoic-Lower Palaeozoic, Democratic Republic of Congo. South African Journal of Geology 106, 47-64.

Wendorff, M., 2003b. Conglomerates and sedimentary megabreccia (olistostrome) in Roan-Mwashya succession in Mufulira, Copperbelt of Zambia. In: Contributions presented at the 3rd IGCP-450 Conference, Proterozoic Sediment-hosted Base Metal Deposits of Western Gondwana; Conference and Field Workshop Lubumbashi 2003, Lubumbashi, D.R. Congo, 94-97.

_____oOo_____